



Cite this: *Environ. Sci.: Processes Impacts*, 2019, **21**, 1280

Overview of HOMEChem: House Observations of Microbial and Environmental Chemistry†

D. K. Farmer, ^a M. E. Vance, ^b J. P. D. Abbott, ^c A. Abeleira, ^a M. R. Alves, ^d C. Arata, ^e E. Boedicker, ^a S. Bourne, ^f F. Cardoso-Saldaña, ^f R. Corsi, ^g P. F. DeCarlo, ^{hi} A. H. Goldstein, ^{ej} V. H. Grassian, ^d L. Hildebrandt Ruiz, ^f J. L. Jimenez, ^k T. F. Kahan, ^{lm} E. F. Katz, ^h J. M. Mattila, ^a W. W. Nazaroff, ^j A. Novoselac, ^q R. E. O'Brien, ⁿ V. W. Or, ^d S. Patel, ^b S. Sankhyan, ^b P. S. Stevens, ^o Y. Tian, ^e M. Wade, ^f C. Wang, ^c S. Zhou, ^l and Y. Zhou^p

The House Observations of Microbial and Environmental Chemistry (HOMEChem) study is a collaborative field investigation designed to probe how everyday activities influence the emissions, chemical transformations and removal of trace gases and particles in indoor air. Sequential and layered experiments in a research house included cooking, cleaning, variable occupancy, and window-opening. This paper describes the overall design of HOMEChem and presents preliminary case studies investigating the concentrations of reactive trace gases, aerosol particles, and surface films. Cooking was a large source of VOCs, CO₂, NO_x, and particles. By number, cooking particles were predominantly in the ultrafine mode. Organic aerosol dominated the submicron mass, and, while variable between meals and throughout the cooking process, was dominated by components of hydrocarbon character and low oxygen content, similar to cooking oil. Air exchange in the house ensured that cooking particles were present for only short periods. During unoccupied background intervals, particle concentrations were lower indoors than outdoors. The cooling coils of the house ventilation system induced cyclic changes in water soluble gases. Even during unoccupied periods, concentrations of many organic trace gases were higher indoors than outdoors, consistent with housing materials being potential sources of these compounds to the outdoor environment. Organic material accumulated on indoor surfaces, and exhibited chemical signatures similar to indoor organic aerosol.

Received 15th May 2019
Accepted 19th June 2019

DOI: 10.1039/c9em00228f

rsc.li/espi

Environmental significance

This article provides an overview of a comprehensive indoor chemistry experiment that was designed to investigate the gas, particle and surface chemistry of a test house. As humans spend on average 90% of their lives in the built environment, indoor chemistry has the potential to affect human health and wellbeing. This study highlights the diverse sources and high concentrations of indoor VOCs and other trace gases, contributions of cooking to indoor organic aerosol, chemical similarities between indoor aerosol and surface films, and indoor concentrations of photolabile molecules.

^aDepartment of Chemistry, Colorado State University, Fort Collins, CO, USA 80523.
E-mail: delphine.farmer@colostate.edu

^bDepartment of Mechanical Engineering, University of Colorado Boulder, Boulder, CO, USA 80309

^cDepartment of Chemistry, University of Toronto, Toronto, ON, Canada M5S 3H6

^dDepartment of Chemistry and Biochemistry, University of California San Diego, La Jolla, CA 92093, USA

^eDepartment of Environmental Science, Policy, and Management, University of California, Berkeley, CA 94720, USA

^fCenter for Energy and Environmental Resources, The University of Texas at Austin, Austin, TX, USA 78758

^gMaseeh College of Engineering & Computer Science, Portland State University, Portland, OR, USA 97201

^hDepartment of Chemistry, Drexel University, Philadelphia, PA 19104, USA

ⁱDepartment of Civil, Architectural and Environmental Engineering, Drexel University, Philadelphia, PA 19104, USA

^jDepartment of Civil and Environmental Engineering, University of California, Berkeley, CA 94720-1710, USA

^kDepartment of Chemistry and Cooperative Institute for Research in Environmental Sciences (CIRES), University of Colorado, Boulder, CO 80309, USA

^lDepartment of Chemistry, Syracuse University, Syracuse, NY 13244, USA

^mDepartment of Chemistry, University of Saskatchewan, Saskatoon SK, Canada S7N 5C9

ⁿDepartment of Chemistry, College of William and Mary, Williamsburg, VA, USA 23185

^oO'Neill School of Public and Environmental Affairs and Department of Chemistry, Indiana University, Bloomington, IN, USA 47405

^pDepartment of Atmospheric Sciences, Colorado State University, Fort Collins, CO, USA 80523

^qDepartment of Civil, Architectural and Environmental Engineering, University of Texas at Austin, Austin, TX, USA 78712

† Electronic supplementary information (ESI) available. See DOI: [10.1039/c9em00228f](https://doi.org/10.1039/c9em00228f)



1. Introduction

In the US, people spend an average of almost 90% of their time indoors, most of that in their own home.¹ As a result, integrated exposures to most airborne pollutants for individuals is strongly influenced by their own household conditions.² Most air quality regulations focus on outdoor air pollution, and most atmospheric chemistry research over the past decades has focused on outdoor air. While air quality research has resulted in a deeper understanding of the sources, concentrations and fates of particles and trace gases in the urban, regional, and global atmosphere, far less is known about indoor air composition and associated chemistry. Indoor environments have distinct air composition from local outdoor conditions. Emissions from indoor sources combine with large surface area-to-volume ratios, relatively short residence times, and lower-than-daytime light levels to yield chemistry indoors that can follow different pathways from dominant processes in the outdoor environment. Most research, monitoring and regulatory programs do not capture these major influences on the air we breathe.

Gases and particles can be categorized according to primary and secondary sources. Primary components are directly emitted from sources, whereas secondary species are produced through chemical reactions in the air (or on surfaces) from precursor molecules. Indoor primary sources include these major categories: the building itself (e.g. wood, linoleum, plastics),^{3,4} consumer products (e.g. personal care products, cleaning or cooking products,⁵ equipment and office products, off-gassing from items brought into the home),^{6,7} microbial⁸ and human⁹ metabolic emissions, occupant activities (e.g. cooking),^{10,11} and intentional (via window opening or ventilation systems) or unintentional (infiltration via leaks in the house envelope) transport of outdoor air into the house. Chemistry occurring inside the house is a secondary source of gases and particles. Chemical processes include gas phase oxidation, partitioning of semi-volatile species among gas and condensed phases, and multiphase chemistry occurring on or in surfaces, in airborne particles or on dust.^{12,13} Molecules can also be emitted into air after being produced within surface materials or other components of the house. Chemistry takes place in and on the organic and aqueous films that cover interior surfaces of buildings. Key sinks for trace gases and particles in indoor air typically include deposition to indoor surfaces, reaction in the gas or particle phase to form altered molecules, and removal from the house by ventilation to the outdoor atmosphere.¹⁴ Accumulation in poorly coupled spaces of a house (e.g. wall cavities) may constitute either permanent or temporary sinks. Ongoing indoor-outdoor air exchange carries with it the chemical composition of the associated air parcels and so influences both indoor and outdoor air quality. Recent studies have shown that volatile chemical products that can be released from indoors, including solvents and personal care products, are increasingly relevant to outdoor aerosol and ozone formation in urban environments.^{15,16}

Real-time instrumentation for outdoor atmospheric chemistry field studies includes both mass spectrometry and

spectroscopy techniques. When applied to indoor air, these instruments can elucidate chemical mechanisms in built environments.^{17,18} For example, direct spectroscopic measurements have demonstrated the importance of NO_3 radicals as indoor VOC oxidants only under high O_3 conditions.¹⁹ Mass spectrometry measurements demonstrated consistently elevated gas phase nitrous acid (HONO) indoors relative to outdoors, indicating the influence of indoor HONO sources and suggesting that HONO could be an indoor OH radical precursor.²⁰ However, spectral radiometry measurements suggest that indoor lighting produces very low photon fluxes, calling into question the potential indoor production of OH.²¹ Aerosol mass spectrometry measurements have demonstrated that occupants can contribute to secondary organic aerosol,²² and that revolatilization of cigarette smoke components can partition to aqueous indoor aerosol particles, producing 'third hand smoke'.²³ Such indoor field studies are frequently observational, although deliberate perturbations (e.g. smoking cigarettes, adding ozone via generators) are sometimes incorporated to answer specific questions.

Studies with real-time instrumentation have provided some important insights into specific processes that occur indoors. Given that humans spend a significant fraction of time in their homes and at work or school, further work is needed to probe these chemical environments. Much of the challenge is driven by the range of indoor sources and chemical reactions, as well as the wide variation in building types and uses. Comprehensive studies of indoor spaces are needed to better understand the range of chemical and microbial environments that humans experience daily. Here, we describe the House Observations of Microbial and Environmental Chemistry (HOMEChem) study, a large-scale collaborative experimental investigation probing deeply into indoor air composition and chemistry with an array of chemical instrumentation that is unprecedented in studying indoor environments. HOMEChem focused on the gas, aerosol and surface chemistry of a test house during simulated everyday activities. The experimental design aims to bridge the space between observational field experiments and controlled chamber studies, and is perhaps best described as a field perturbation experiment. Outdoor conditions and natural fluctuations in meteorology and building parameters were allowed to influence the sources and sinks of indoor air, but indoor activities were carefully prescribed with an emphasis on cooking, cleaning and variations in occupancy. This paper describes major features of the research campaign, including the experimental design and test house characteristics. Illustrative results are presented. More detailed assessments of particular aspects of the research campaign will be described in future publications.

2. Methods

The HOMEChem study took place over four weeks, 1–28 June 2018, at the UTest House on the J. J. Pickle Research Campus of the University of Texas at Austin. The UTest House is a 3-bedroom, 2-bathroom manufactured home (Fig. 1 and S1–S5;† floor area 111 m²; volume 250 m³). The house has two



separate heating ventilation and air conditioning (HVAC) systems with underfloor and overhead air diffusers, respectively; only the overhead ceiling system, which provided more rapid mixing during air conditioning, was employed in this study. As the focus of the HOMEChem experiment was to capture chemical processes driven by human activities rather than variable building factors, throughout most of the campaign the HVAC system was operated to maintain as constant conditions as possible for the indoor thermal environment and ventilation rate.

2.1 House ventilation and household state monitoring

A dedicated outdoor air supply system was operated to keep the house positively pressurized relative to outdoors whenever the doors and windows were closed so as to minimize temporal variations in house ventilation rate driven by temperature differences and wind. This system delivered a constant outdoor air flow, which provided an average \pm standard deviation air change rate (ACR) of $0.5 \pm 0.1 \text{ h}^{-1}$ when the doors and windows were closed. This outdoor air was supplied into the house near the return of the air handling unit of the HVAC system. Thus, incoming outdoor air was mixed with the room air at the air handling unit's return, and then conditioned by the HVAC system before being dispersed through the house.

Apart from providing mechanical ventilation, major elements of the UTest House HVAC system are representative of a typical residential system, providing cooling, dehumidification and air circulation functions. For the HOMEChem

campaign, the fan in the air handler of the HVAC system was set to operate continuously, regardless of heating or cooling demand, moving air through the HVAC system at a flow rate of $2000 \text{ m}^3 \text{ h}^{-1}$ (equivalent to 8 house volumes per hour) so as to provide consistently rapid mixing throughout the house. A thermostat controlled the on/off cooling functions of the HVAC system as needed to maintain air temperature within the desired range. The filters in the outdoor air supply and air handling unit were removed to prevent measurements from being affected by filter type and filter conditions. As a consequence of the absence of an HVAC filter, indoor concentrations of particles and reactive trace gases during unperturbed, background periods may be somewhat higher than would have been the case in the presence of a filter. The exhaust hood above the stove was not operated during this study.

To facilitate internal air mixing, all interior doors were kept open throughout the HOMEChem study; the only exceptions were doors to both bathrooms and all closets, which were kept closed. Volunteers used only the master bathroom during experiments. The exhaust fan in this bathroom was kept on during the entire campaign to ensure that air entering the bathroom exited through the fan to the outside, thus minimizing emissions of stored cleaning products from entering the house air space. To enhance mixing in the living and kitchen area, a ceiling fan in the living room was on during the entire campaign. During experiments, all outside doors and windows were closed unless specified otherwise.

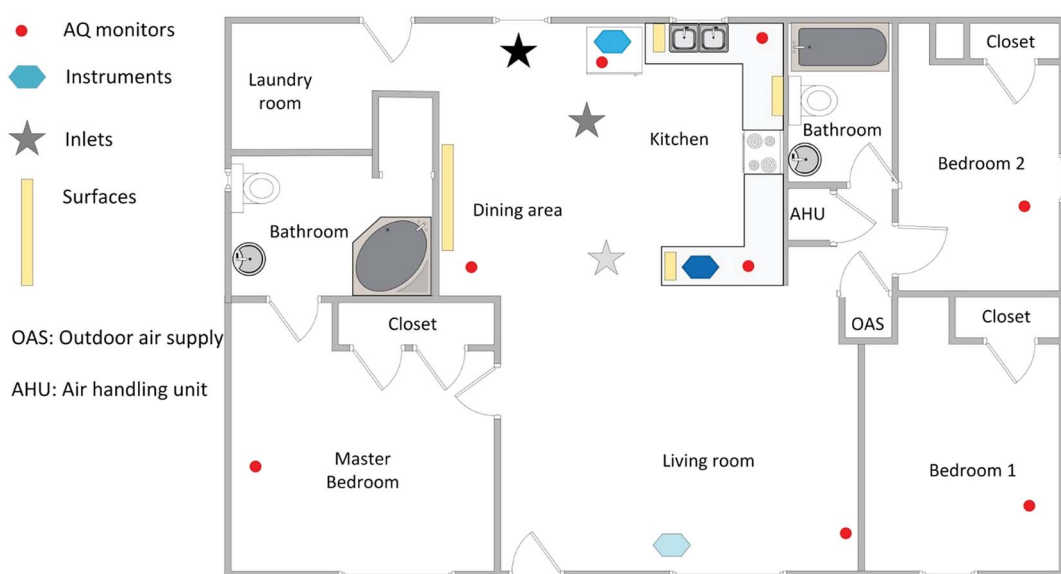


Fig. 1 The UTest house floor plan includes a large open living room and kitchen space, including a sink and stove. The markers indicate instrument/inlet general locations. The bathroom doors were sealed with the master bathroom's exhaust fan left on; all other interior room doors were kept open. Three sets of large instruments were maintained inside the house (light blue hexagon in living room: HO_x , HONO and spectral radiometer measurements; medium blue hexagon in kitchen: NH_3 measurement; dark blue hexagon between kitchen and living room: aerosol and biological aerosol size distribution measurements). Low-cost air quality monitors were placed on top of the cupboards separating the kitchen from the living room area, and in the living room and bedrooms (red circles). Multiple vertical sampling surfaces were placed in the dining area and kitchen (yellow bars). Inlets for external sampling were located in the kitchen area (stars; black: SVTAG inlet; light grey: O_3 , NO_x , SO_2 , CO_2 and GC measurements of VOCs; medium grey: all other measurements). The locations of the outdoor air supply and air handling unit are indicated. The dishwasher is under the counter to the left of the sink, and the refrigerator between the sink and SVTAG inlet.



The test house was outfitted with 39 wireless sensors (see Table S3† for locations; SmartThings, Inc., Mountain View, CA, USA) to monitor motion, window/door open/closed status, and appliance usage. Data loggers recorded temperature in the kitchen and relative humidity (Veris HD2XVSX sensor, accuracy $\pm 2\%$ between 10 and 80% RH) in the living room. Additional sensors measured air temperature and CO₂ levels in all rooms, and temperature and relative humidity at the inlet of the air handling unit, in the air supply duct after the air handling unit, and in the outdoor supply air. We also measured interior surface temperatures at 40 locations on the walls, floor and ceiling (Omega 44033 thermistor; accuracy of $\pm 0.1\text{ }^{\circ}\text{C}$). Spectrally-resolved solar irradiance was measured with an Ocean Optics USB4000 (1 minute average, <15% error; fiber optic cable coupled with a cosine corrector), and alternated measurements between the living room and kitchen windows. Additional experiments investigated the spatial variability of light intensity and the contributions of diffuse and reflected light on total indoor spectral irradiance.

The air conditioning (AC) setpoint temperature was 25 °C for the kitchen and living area throughout the study period with the exception of a few specified periods with either no AC or a higher setpoint. Large occupancy and intensive cooking events, combined with heat gain from outdoors, sometimes exceeded the cooling capacity of the AC system and sporadically caused increases in indoor temperature above the setpoint. In addition to cooling, the air conditioning coils provided dehumidification through condensation when the thermostat called for cooling. An additional small-capacity dehumidifier positioned in series with the air handling unit provided continuous dehumidification, helping to prevent large variations in relative humidity. During experimental days, the kitchen and living area temperature was $25 \pm 2\text{ }^{\circ}\text{C}$ (average \pm standard deviation) and the RH was $57 \pm 6\%$. When windows and doors were opened and the air conditioner was turned off, the indoor temperature was $31 \pm 3\text{ }^{\circ}\text{C}$. Throughout the entire HOMEChem study, indoor temperature ranged from 23 °C to 36 °C, while the relative humidity (RH) ranged from 43% to 82%. In contrast, outdoor temperature ranged from 20 °C to 38 °C (average \pm standard deviation of $29 \pm 4\text{ }^{\circ}\text{C}$) and RH ranged from 36% to 98% ($71 \pm 17\%$) during HOMEChem.

2.2. HOMEChem experimental design

HOMEChem experiments followed two approaches: sequential experiments and layered experiments. Sequential experiments repeated similar activities throughout the day, interspersed with periods of enhanced ventilation *via* window opening. Sequential experiments aimed to investigate emissions and short-term chemical processes following specific, isolated activities. Layered experiments included different cooking and cleaning activities performed throughout the day with no interspersed window opening. Layered experiments allowed emissions from multiple activities to interact in the house over longer periods of time. Layered experiments were designed around scripts to simulate real-life use of a home. The major event types investigated during HOMEChem were cooking,

cleaning, and variable human occupancy (including the use of personal care products). Ventilation rates were also deliberately manipulated in some experiments through the opening and closing of doors and windows.

We combined the experiment types into six day-long categories: (1) unoccupied background, (2) sequential experiments (cooking, cleaning, occupancy, ventilation), (3) layered experiments, (4) Thanksgiving, (5) maintenance, and (6) open house (one day) (Fig. 2). Unoccupied days involved no perturbation to the house, with no volunteers or researchers entering the house. Maintenance days typically included specific tests or additional experiments. Detailed schedules are provided in the ESI† (§S6).

The sequential ventilation experiments of 4 June entailed seven replicates of two steps: (i) opening doors and windows and operating several household box fans; (ii) after 30 minutes, closing windows and doors, turning off fans and leaving the house unoccupied for 90 minutes. For cooking and cleaning sequential days, in which each perturbation activity (e.g. mopping or stir-fry) typically lasted 10–40 minutes, we opened doors and windows two hours after the start of the activity, closed them after 30 minutes, and then waited another 30 minutes before repeating the activity.

For sequential cooking experiments, the experimental meal was a vegetable stir-fry. Volunteers cooked the stir-fry four times per day on three days, alternating between a propane stove and an electric hot plate as heat sources, and an aluminum wok and cast iron skillet as cooking surfaces. For sequential cleaning experiments, volunteers mopped the vinyl floors in the kitchen and living room with four cleaning products: (1) a commercial bleach solution, (2) a commercial product advertised as “all natural”, (3) a pine-scented commercial product, and (4) a vinegar solution. Volunteers preceded or followed the vinegar mopping with wiping windows, tables, and countertops using an ammonia solution. Different volunteers conducted replicated activities following detailed instructions regarding volume of vegetables, sauce and rice cooked; cooking temperature and time; and time spent mopping. Volunteers mixed the cleaning solvents according to manufacturer's instructions, and weighed mopping solutions before and after mopping.

The three staggered occupancy days followed a different schedule from other sequential experiments. Up to 12 occupants entered the house in groups of 2–3 at 15 minute intervals. After 75 minutes, the volunteers left in the same order they entered, creating a stepwise increase and decrease in total occupancy (Fig. 3). After a two-hour break with windows and doors open to ventilate the house, volunteers repeated the experiment. On the first occupancy day, volunteers wore minimal personal care products, opting for products advertised as ‘all natural’ or ‘organic’. On the second occupancy day, volunteers wore their ‘usual’ quantities and types of products. On the third day, volunteers wore generous (but not unrealistic) amounts and types of personal care products.

Layered experiments involved three volunteers cooking, cleaning and occupying the house for 9.5 hours without opening the doors or windows. The layered day followed a prescribed schedule of cooking breakfast, mopping the floors with a terpene cleaner, cooking lunch, wiping the kitchen





June						
M	T	W	T	F	S	S
				1 Shake-down	2 Unoccupied background	3 Maintenance
4 Sequential ventilation	5 Sequential terpene cleaning I	6 Sequential stir-fry I	7 Sequential bleach cleaning I	8 Layered I	9 Maintenance	10 Sequential bleach cleaning II
11 Staggered occupancy I	12 Sequential stir-fry II	13 Sequential natural product cleaning I	14 Maintenance	15 Unoccupied background	16 Maintenance	17 Sequential stir-fry III
18 Thanksgivings I	19 Layered II	20 Sequential natural product cleaning II	21 Layered III	22 Open House	23 Maintenance / O ₃ addition	24 Staggered occupancy II
25 Layered IV	26 Sequential ammonia/ vinegar cleaning	27 Thanksgivings II	28 Staggered occupancy III			

Fig. 2 Experimental schedule for HOMEChem.

counter surfaces with commercial 'bleach free' wipes, making coffee and toast, cooking dinner, operating the dishwasher, mopping with a bleach solution, and exiting the house. Similar to the primary layered experiments, Thanksgiving days simulated the traditional American holiday activity with four volunteers cooking a turkey dinner with trimmings for 10+ additional volunteers, who arrived, ate and cleaned up. On maintenance days, researchers calibrated instruments and ran additional experiments (e.g. instrument intercomparisons). During the Open House, 40+ individuals visited the HOMEChem site and entered the test house, with no specific experiments performed on that day. Exact numbers of attendees and the times of their presence indoors were not recorded during the open house event.

Volunteers conducted supplemental experiments during evenings and on maintenance days. These included particle-generation events (e.g. cooking toast on the evening of 26 June; releasing Arizona test dust on the evenings of 22 and 28 June), ozone addition experiments (three experiments on the night of June 23 and three experiments on the night of June 24), and a temperature ramp (house temperature setpoint ramped from 24.4 °C down to 17.8 °C and back to 24.4 °C over the course of nine hours on June 28–29).

All major appliances were installed in the UTest house more than a year prior to HOMEChem. The oven had been unused until May 2018.

2.3 Volunteer information

Researchers from the HOMEChem science team performed all activities. An experimental log retains time-dependent numbers of occupants, but identities and any potentially identifying information (e.g. age, gender) of volunteers are not available. Volunteers recorded personal care products used only during sequential occupancy experiments. The Institutional Review

Board's (IRB) human research review was waived for the HOMEChem study because the only data recorded was the number of occupants in the house and the types of personal care products used in sequential occupancy experiments, with no ties to personal identifying information.

2.4 Chemical measurements

The HOMEChem study included an array of real-time instruments with inlets measuring both indoor and outdoor air (Tables 1–4). Table 5 summarizes off-line sample collection for surface composition, passive sampling and aerosol chemistry. The study also included seven different low-cost air quality monitors (five commercially available and two research prototype units), with replicated monitors deployed in different locations throughout the house (ESI Table S2†).

3. Case studies

The HOMEChem dataset provides a wealth of information on not only trace gas and particle concentrations inside and outside the test house, but also surface composition and the role of typical activities in altering this chemistry. A complete synthesis of HOMEChem data is beyond the scope of this initial overview. Instead, we describe several case studies that demonstrate the utility of this dataset for investigating indoor chemistry in a residential environment. The first case study contrasts indoor and outdoor concentrations of trace gases, particles and photolysis rates, providing chemical context for the HOMEChem study. The second case study demonstrates cooking as a substantial, yet chemically diverse, source of indoor particles. The third case study highlights the complexity of multiple sources in contributing to VOCs in general, and organic acids in particular. The fourth case study highlights new opportunities in indoor chemistry

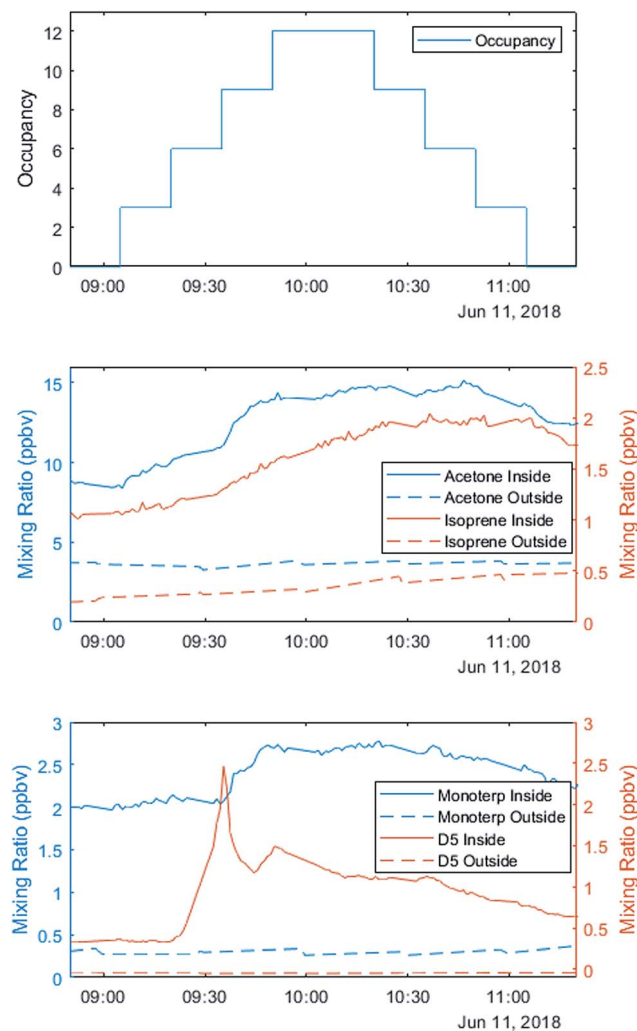


Fig. 3 Occupancy was staggered on the three sequential occupation experiments. The first occupancy period on 11 June (minimal personal care product day) exemplifies the enhancement of acetone, isoprene, monoterpenes and the D5-siloxane from human emissions.

measurements by comparing multiple methods for characterizing films deposited on indoor surfaces. The fifth case study demonstrates the challenges of measuring even relatively abundant trace gases, specifically NO_2 , in chemically complex indoor air.

3.1 Case study 1: contrasting indoor vs. outdoor air

Differences observed between indoor and outdoor air composition were generally consistent with findings in previous studies. For example, with the exception of periods impacted by cooking events, accumulation mode particle concentrations were lower indoors than outdoors during HOMEChem (Fig. S6 and S10†). However, indoor particle concentrations were markedly elevated during cooking events, for example reaching hundreds of $\mu\text{g m}^{-3}$ during stir-fry events. Whereas accumulation mode particles commonly dominate the $\text{PM}_{2.5}$ aerosol mass concentration (*i.e.* mass of particles with diameter $<2.5 \mu\text{m}$) in the outdoor environment, ultrafine (*i.e.* $<100 \text{ nm}$; $\text{PM}_{0.1}$)

particles can be so numerous indoors during cooking events that they influence $\text{PM}_{2.5}$.

In the absence of ozone generating devices, O_3 has long been known to be lower indoors than outdoors – and HOMEChem data are no exception.^{51,52} Fig. 4 compares indoor and outdoor distributions of O_3 and other inorganic trace gases. As most of the data points were collected during unoccupied, unperturbed conditions, peaks in the histogram for indoor data represent baseline conditions. Outdoor O_3 levels varied through the diel cycle, peaking in the mid-afternoon, consistent with photochemical generation typically encountered in urban environments. Ozone was consistently lower indoors than outdoors (Table 6). Under closed-house conditions, O_3 exhibited a relatively steady mixing ratio of $5 \pm 3 \text{ ppb}$ independent of time of day, increasing only when the house was opened or when O_3 was deliberately injected. At night, outdoor O_3 reached minima of $10\text{--}15 \text{ ppb}$, two to three times larger than the concurrent indoor mixing ratio.

In contrast to O_3 , several other trace gases (*i.e.* NO_x , CO , CO_2) were typically higher indoors than outdoors (Table 6). These compounds were clearly influenced by indoor activities, increasing when the gas stove or oven was in use, and, in the case of CO_2 , from metabolic emissions when humans occupied the house. During the Thanksgiving experiments, NO reached a maximum of 1085 ppb , NO_2 rose to 105 ppb and CO_2 peaked at slightly above 4000 ppm . The elevated NO_2 levels are comparable to the 1 hour 100 ppb outdoor air quality standard set by the US EPA, although we note that these concentrations only persisted for short periods (minutes to hours) during HOMEChem. Indoor CO (range of 0.1 to 10.2 ppb) was higher than outdoor (range of 0.1 to 2.4 ppb). Indoor enhancements in CO and NO_x were likely due primarily to stove/oven use and the associated gas pilot lights. Indoor CO never exceeded the NAAQS 1 hour average limit of 35 ppm or 8 hour average limit of 9 ppm .

Background (unoccupied, unperturbed) indoor NO and NO_2 mixing ratios were similar ($5.2 \pm 6.4 \text{ ppb}$ NO and $5.5 \pm 2.1 \text{ ppb}$ NO_2). The much higher $\text{NO} : \text{NO}_2$ ratio indoors than outdoors is consistent with most of the indoor NO_x originating as NO emitted from the gas stove and oven pilot lights. Outdoors, NO would rapidly reach a steady-state with NO_x dominated by NO_2 , but the low indoor O_3 concentrations enable the relatively high indoor $\text{NO} : \text{NO}_2$ ratio to persist. The high indoor $\text{NO} : \text{NO}_2$ ratios during cooking events contrast to older reports of relatively high emissions of NO_2 from gas stoves, but we note that reported emission ratios of $\text{NO} : \text{NO}_2$ from indoor combustion sources span a large range.^{53–55} Higher $\text{NO} : \text{NO}_2$ ratios have been observed from gas-powered appliances in more recent studies.^{56,57} Appliance design may have changed resulting in higher $\text{NO} : \text{NO}_2$ emissions, or differences may be driven by measurement technology: older measurements often utilized catalytic NO_2 converters that are subject to interferences from HONO , PAN , HNO_3 and other oxidized nitrogen compounds.⁵⁸ High indoor NO_x and CO_2 and low O_3 (relative to outdoor concentrations) are consistent with previous residential studies in the US.^{59–62}



Table 1 Summary of instruments for inorganic gas phase measurements^a

Measured species	Sampling location	Instrument	Time resolution	Uncertainty	Notes
O ₃	Alternating living room & outdoors	2B Technologies model 202	10 s	LOD: 1.2 ppb Error: 5%	Two 6-point calibrations during HOMEChem with 2B Technologies model 306 O ₃ generator Inlet lengths: 17.3 m indoor, 8.6 m outdoor
O ₃	(i) House air return (ii) House air supply	2× Horiba APOA 370 ambient ozone monitor	10 s	LOD: 0.5 ppb	Cross flow modulation type, non-dispersive ultraviolet absorption method
NO, NO ₂	Alternating living room & outdoors	Thermo Fisher model 42i TL with home-built blue light converter for NO ₂ detection	2 min	LOD: 2.3 ppb Error: 5%	Calibrated using external 11-point calibration for 0–600 ppb range Inlet lengths: 17.3 m indoor, 8.6 m outdoor
NO ₂	Living room	Environnement, S.A. Cavity attenuated phase shift spectroscopy (CAPS) NO ₂ monitor ²⁴	1 min	LOD: 0.1 ppb	Linearity checks before and after campaign, calibration after campaign. Details in ESI Section 7
NH ₃	Kitchen	Picarro G2103	1 min	LOD: 0.5 ppb Error: 5%	Instrument calibrated by Picarro immediately prior to deployment
SO ₂	Alternating living room & outdoors	Teledyne LIP	1 min	LOD: 0.05 ppb Error: 5%	Internal low and high span calibrations with SO ₂ cylinder; see ESI Section 5 for additional details Inlet lengths: 18.4 m indoor, 7.9 m outdoor
CO ₂	Alternating living room & outdoors	LICOR model LI- 840A	1 s	LOD: 10.2 ppm Error: 4%	Internal low and high span calibrations for 0–6500 ppm during HOMEChem. External post-campaign 9-point calibration Inlet lengths: 18.4 m indoor, 7.9 m outdoor
CO, CO ₂ , CH ₄	Alternating kitchen & outdoors *Inlet shared with HR-AMS	Picarro G2401	1 min	Uncertainty CO ₂ < 50 ppb CO < 2 ppb CH ₄ < 1 ppb	Instrument calibrated prior to deployment and upon return Inlets: 9.5 mm (3/8") o.d. stainless steel tubing
CO ₂ , H ₂ O	Alternating kitchen & outdoors	LICOR model LI-840A	1 s	LOD CO ₂ : < 1 ppm H ₂ O: < 10 ppm	Inlet lengths: <0.5 m of PFA Teflon tubing in addition to inlet tubing described in the EESI-ToF-MS description (Table 3)
HO ₂ , HO ₂ ^{*b}	Living room window	LIF FAGE ^{25,26}	1 min	LOD: 1 × 10 ⁷ molec per cm ³	Calibrated using water vapor photolysis method before, during, and after campaign
OH, HONO	Living room window	LP/LIF-FAGE ²⁵	15 min	LODs OH: 1 × 10 ⁶ molec per cm ³ HONO: 50 ppt	OH calibrated using water vapor photolysis method before, during, and after campaign. HONO calibrated before and after campaign

^a All gas phase inlets were made of 0.635 cm (1/4") o.d. PFA tubing unless stated otherwise. Alternating sampling locations were controlled by integrated valve switching, typically 25 minutes indoors followed by 5 minutes outdoors. ^b HO₂^{*} refers to the sum of HO₂ radicals plus a fraction of certain RO₂ radicals.²⁷

Indoor and outdoor concentrations of CH₄ were similar (ranges 1.8–2.4 ppm indoors and 1.8–2.7 ppm outdoors) with no clear diel cycle. Similarly, sulfur dioxide (SO₂) showed no diel cycle or differences in indoor and outdoor concentrations. Indoor SO₂ peaked at 11.5 ppb on 27 June during the Thanksgiving experiment. Gas stoves and matches are known sources of particulate sulfate, and are likely indoor SO₂ sources during HOMEChem.⁶³

Spectral irradiance, and thus photolysis rate constants, are substantially lower indoors than outdoors. For example, HONO photolysis rate constants (J_{HONO}) are typically 1–2 orders of

magnitude lower indoors than outdoors at any given time. Indoor temporal trends in photon fluxes and photolysis rates depend on solar zenith angle, presence of clouds, and placement of windows, causing strong spatial heterogeneity and differences in diel patterns not only between indoor and outdoor environments, but also among different locations indoors (Fig. 5). These spatial gradients may influence photolysis rates for photolabile molecules such as NO₂. The resulting photochemical production of O₃ is likely less than the physical supply by transport of outdoor air under most conditions, but the irradiance and NO₂ measurements suggest both spatial and



Table 2 Summary of instruments for organic gas phase measurements, including instruments that measure semi-volatile components in the particle phase^a

Measured quantity	Sampling location	Instrument	Time resolution	Notes
VOCs	Living room	VOC 4-channel GC ²⁸	50 min	C_2-C_8 hydrocarbons; BTEX; speciated monoterpenes (limonene, α -pinene, β -pinene); CFCs; C_1-C_5 alkyl nitrates Daily two-point calibrations with multi-component whole air standards. Inlet lengths: 13.2 m
VOCs	Alternating kitchen & outdoors	PTR-TOF-MS ^{4,29}	1 min	Target species directly calibrated; all other species concentrations calculated based on theoretical transmission Inlet lengths: 8.4 m
Oxidized VOCs, halogenated species, N_2O_5	Alternating kitchen & outdoors	Iodide CIMS ³⁰	1 s	On-line calibration of formic, acetic, propionic, butyric, and pentanoic acid using permeation tubes Off-line calibrations include Cl_2 , $ClNO_2$, $HOCl$, N_2O_5 , multiple organic acids Inlet lengths: 7 m indoor, 5 m outdoor
Organic acids, HONO	Alternating kitchen & outdoors	Acetate CIMS ²⁰	1 s	Calibrated species: $HONO$ ³¹ ; $HNCO$ ³² ; formic, propionic, butyric, and pentanoic acid (<i>via</i> permeation tubes) Inlet lengths: 10 m indoor, 8 m outdoor, shared inlet with iodide CIMS
Gas and particle composition and partitioning	Kitchen (switched to outdoors on a few nights)	FIGAERO-CIMS ³³ with iodide ionization	1 s gas phase; 1 h for particle phase 1 h	Inlet lengths: 2.1 m outdoor, 8.4 m indoor (PFA for gases, 9.5 mm o.d. stainless steel tubing for particles) Calibrated by aerosol spray for levoglucosan, malonic acid and by drops onto FIGAERO filter for multiple organic acids Calibration <i>via</i> internal standards and >100 authentic external standards 20 minute sampling window through stainless steel tubing (16 mm (5/8") o.d.; inlet lengths 2 m indoor, 3.7 m outdoor)
Gas and particle phase semi-volatile organic compounds	Alternating kitchen & outdoors	SV-TAG: thermal desorption aerosol gas chromatography with online derivatization ^{11,34}		

^a All gas phase inlets were made of 0.635 cm (1/4") o.d. PFA tubing unless stated otherwise. Alternating sampling locations were controlled by integrated valve switching, typically 25 minutes indoors followed by 5 minutes outdoors.

temporal variability in O_3 production rates in the indoor environment.

3.2 Case study 2: indoor $PM_{2.5}$ and cooking

Cooking activities were the primary source of indoor submicron particles during HOMEChem. While particle emissions from cooking have been studied extensively, a major focus has been on particles from solid fuel combustion (*e.g.* biomass and coal), which are still used by more than a third of the world's population.^{65,66} In developed countries, cleaner cooking fuels, such as natural gas, propane, and electricity, emit less particle mass compared to solid fuels. Nevertheless, cooking is a well-known indoor particle source.^{67,68} High particle mass concentrations were observed during HOMEChem cooking activities, relative to outdoor levels. The maximum size-segregated particle mass concentrations (*i.e.* $PM_{0.1}$, $PM_{0.5}$, PM_1 , $PM_{2.5}$, PM_{10} , and PM_{20}) observed during each meal highlight the variation with cooking type (Fig. 6a). The highest particle mass concentrations on layered days occurred during breakfast. The $PM_{2.5}$ level exceeded 200 $\mu\text{g m}^{-3}$, with fine particles accounting for >70% of the

total observed particle mass. The smaller size modes, $PM_{0.1}$ and $PM_{0.5}$, were also substantially elevated, exceeding 30 $\mu\text{g m}^{-3}$ and 170 $\mu\text{g m}^{-3}$, respectively, during breakfast preparation. (These mass concentrations are derived from number-based measurements using the SMPS and APS.) Fig. 6a assumes a single particle density of 1 g cm^{-3} , consistent with hydrocarbon-like organic aerosol, although atmospheric aerosol density varies from 0.9–1.8 g cm^{-3} depending on composition. Of course, these reported values represent only one house with a particular pattern of cooking under a single set of ventilation conditions.

Different cooking activities resulted in different particle size distributions (Fig. 6b). Particles less than 20 nm in diameter dominated the number size distributions during cooking with the stove, oven, or hot plate, consistent with previous measurements.⁶⁹ Toasting bread in an electric toaster was the only cooking activity in which particle number concentrations were not dominated by particles smaller than 20 nm.

During cooking events, the HR-AMS detected substantial amounts of organic aerosol (often >100 $\mu\text{g m}^{-3}$). Outdoors,



Table 3 Summary of instruments for real-time particle composition measurements^a

Measurement	Instrument	Inlet	Notes
Submicron non-refractory particle composition	HR-AMS ³⁵	Alternating kitchen & outdoors (9.5 mm (3/8") o.d. stainless steel tubing), sample air dried with MD700 Nafion drier	1 min time resolution LOD: $0.312 \mu\text{g m}^{-3}$, $0.024 \mu\text{g m}^{-3}$ (chloride), $0.040 \mu\text{g m}^{-3}$ (sulfate), $0.024 \mu\text{g m}^{-3}$ (nitrate), $0.394 \mu\text{g m}^{-3}$ (ammonium)
Submicron non-refractory particle composition with thermal denuder	TD-TOF-ACSM ³⁶	Alternating kitchen & outdoors (9.5 mm (3/8") o.d. copper tubing)	40 s time resolution LOD: $<0.2 \mu\text{g m}^{-3}$ for particle species
Submicron non-refractory particle composition	ACSM ³⁷	Outdoor inlet (3 m length \times 6.3 mm (1/4") o.d. copper with PM2.5 cyclone and diffusion dryer)	30 min time resolution Sampled indoors from 17–20 Jun and on 26 Jun (8 m of 6.3 mm (1/4") o.d. copper)
Speciated organic aerosol composition	EESI-ToF-MS	Alternating kitchen and outdoors	5 s time resolution LODs: 350 ng m^{-3} for levoglucosan and $1.20 \mu\text{g m}^{-3}$ for oleic acid
Particle absorption in UV-IR	2 \times microAeth MA200 ³⁸	(i) Kitchen (ii) Outdoors	1 min time resolution 5 wavelength UV-IR absorption 1.5 m inlet with diffusion dryer
Black and brown carbon	AE-33 Aethalometer ³⁹	Alternating kitchen and outdoor (inlet shared with HR-AMS, dried with MD700 Nafion drier)	1 min time resolution 7 wavelength UV-IR absorption
Metal content of PM _{2.5}	Aerosol spark emission spectrometer ⁴⁰	Kitchen	2 min to 4 h time resolution

^a Alternating sampling locations were controlled by integrated valve switching, typically 25 minutes indoors followed by 5 minutes outdoors. Time resolution represents final data product.

cooking-associated organic aerosol (COA) can be identified in aerosol mass spectra through ratios of tracer ions and component factor analysis; COA has also been observed to be

transported into the indoor environment from outdoors.^{22,70–72} During HOMEChem, COA size distributions, concentrations, and bulk mass spectral profiles varied considerably with meal

Table 4 Summary of instruments for particle size distribution measurements^a

Size range	Instrument	Inlet location	Notes
1–4 nm	Airmodus A11-nCNC system ⁴¹	Kitchen	5 min per scan
4–105 nm	SMPS (TSI 3080 EC + 3085 nano-DMA + 3788 water CPC)	Kitchen	5 min per scan
11–533 nm	SMPS (TSI 3080 EC + 3081 long-DMA + 3787 water CPC)	Kitchen	5 min per scan
17 nm–580 nm	SMPS (TSI 3080 EC + 3081 DMA + 3075 CPC)	Alternating kitchen and outdoor Inlet shared with EESI-TOF-MS	2.5 min
130 nm–3 μm	4 \times POPs (portable optical particle sensors, Handix Scientific) ⁴²	(i) Kitchen (ii) Living room (iii) Bedroom 1 (iv) Outside (1–23 June) and kitchen counter (24–28 June)	1 s
60–1000 nm	UHSAS (Droplet Measurement Technologies) ⁴³	Alternating kitchen & outdoor inlet Inlet shared with HR-AMS	1 s Likely saturated at concentration $> 3000 \text{ particles cm}^{-3}$
10–946 nm	SEMS (Brechtel Manufacturing incorporated model 2002)	Outdoor	30 min
500 nm–20 μm	2 \times APS (TSI 3321) ⁴⁴	Inlet shared with ACSM (i) Kitchen (ii) Outdoor	1 min per scan Minimum particle count: $0.001 \text{ particles cm}^{-3}$
500 nm–15 μm (fluorescent particles)	UV-APS (Ultraviolet APS, TSI 3314) ⁴⁵	Kitchen	1 min
PM _{2.5}	DustTrak (TSI 8520)	Kitchen (above kitchen cabinets)	1 min. Data collection June 23–29

^a Acronyms: SMPS = scanning mobility particle sizer, EC = electrostatic classifier, DMA = differential mobility analyzer, CPC = condensation particle counter; UHSAS = ultra high sensitivity aerosol spectrometer; SEMS = scanning electrical mobility system; APS = aerodynamic particle sizer.



Table 5 Summary of sample collection and surface chemistry measurements for off-line analysis

Measurement	Surface material/location	Measurement	Notes
Spatially-resolved metabolites and microbial communities ⁴⁶	Multiple surfaces throughout the kitchen living room and bathroom	HPLC MS/MS 16S sequencing	Samples collected on 31 May and 29 June
Passive VOC samplers ⁴⁶	Multiple surfaces throughout the kitchen living room and bathroom	GC/MS	Samples collected on 1 and 29 June
Surface nitrite ²⁰	Glass/dining room	Surface wipes with nylon filter followed by Griess test using UV-vis	Samples collected and analyzed daily
Surface depositions	Glass/dining room	AFM/AFM-IR, Orbitrap MS, ICP-MS	Samples collected after exposure durations of 3 h, 24 h and multiple days
Surface depositions ⁴⁷	Glass & painted drywall substrates in dining area	Functional groups	12 × 24 h samples
Metal content of PM _{2.5} ^{48,49}	Sample collected on 37 mm Teflon filters from inlets installed indoors (kitchen) and outdoors. (Sample train included 2.5 μ m impactor)	Inductively coupled plasma mass spectrometry (ICP-MS)	Indoor samples collected twice daily from 7–28 June; outdoor samples collected from 17–28 June
Surface depositions ⁵⁰	Glass/dining room on the wall and above stove	Offline HR-ToF-AMS and ESI FT-ICR	Samples extracted with acetonitrile
Particle samples	Filter collection	SEM	
Passive SVOC samplers	Sorbent material (PDMS)	GC-MS	Daily sample collection on 18 days

Table 6 Average indoor and outdoor mixing ratios for selected trace gases during HOMEChem

	Indoor mean \pm standard deviation	Outdoor mean \pm standard deviation
O ₃ (ppb)	8 \pm 18	28 \pm 11
NO (ppb)	50 \pm 130	1.7 \pm 1.4
NO ₂ (ppb)	7 \pm 27	5 \pm 3
CO (ppb)	0.4 \pm 0.8	0.1 \pm 0.04
SO ₂ (ppb)	3 \pm 1	2.7 \pm 0.6
CO ₂ (ppm)	670 \pm 530	413 \pm 8
CH ₄ (ppm)	1.90 \pm 0.05	1.88 \pm 0.05

type and preparation method (e.g. gas stove *vs.* hot plate *vs.* toasting *vs.* oven). The high time resolution of the HR-AMS enables differentiation of submicron aerosol composition throughout the cooking process. Many HOMEChem meals involved placing food into hot oil, and one involved splashing water into hot oil to aerosolize oil (“oil splash”). We contrast composition and mass spectra between aerosolized oil (Fig. 7a) and stir-fry COA produced when vegetables are added to the oil (Fig. 7b).

The particles emitted during the oil splash and stir-fry experiments were dominated by organic molecules. Inorganic components (non-refractory nitrate NO₃, sulfate SO₄, chloride

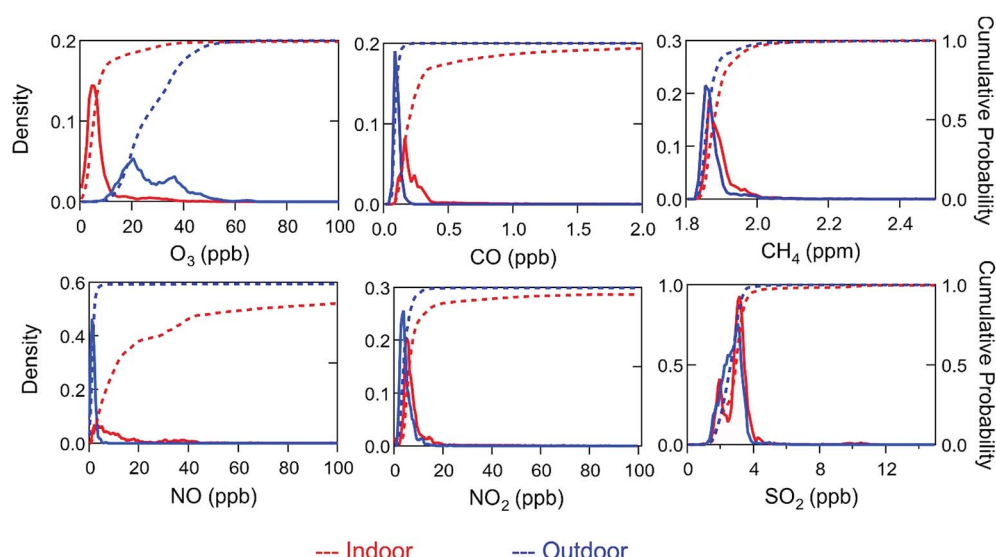


Fig. 4 Normalized probability (solid line; left axis) and cumulative probability (dashed line; right axis) distributions of trace gas data for the entire HOMEChem experiment for indoor (red) and outdoor (blue) measurements. Mixing ratios of O₃ (2B Technologies UV absorption measurement; 10 s averages), CO (Picarro 2401, 1 min average), CH₄ (Picarro 2401, 1 min average), NO (chemiluminescence measurement, 2 min average), NO₂ (blue light converter + chemiluminescence, 2 min average), and SO₂ (pulsed fluorescence measurement, 1 min average).



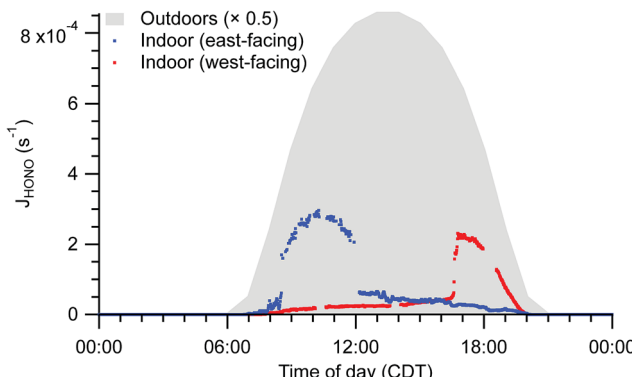


Fig. 5 Indoor photolysis rate constants of HONO calculated from solar spectral photon fluxes measured near to the east-facing and west-facing windows under clear sky conditions. Photon fluxes were determined from measured spectral irradiance. Outdoor HONO photolysis rate constants based on tropospheric ultraviolet and visible (TUV) radiation model results are shaded in grey for comparison.⁶⁴

Chl, and ammonium NH₄) comprised <3% of the average total aerosol signal. Sulfate concentration remained at background levels throughout cooking experiments, trending with outdoor concentrations, while aerosol mass of other inorganic components (NO₃, Chl, NH₄) increased. The C_xH_y⁺ family of organic ions comprised most of the aerosol mass for both the aerosolized oil and the food in stir-fry experiments, followed by C_xH_yO_z⁺ ions, consistent with the fatty acid composition of cooking oils. Slight enhancements in C_xH_yN⁺ and C_xH_yON⁺ were observed in both experiments but contributed little to total particle mass (<1% of the total).

The mass spectra of stir-fry organic aerosol (Fig. 7d) shows a greater contribution of C_xH_yO_z⁺ ions than the oil splash (Fig. 7c), likely due to the complex sugars and proteins originating from the vegetables being cooked and the added stir-fry sauce. The oil splash mass spectrum is dominated by C_xH_y⁺ ions, consistent with a primary source of long-chain

hydrocarbons (e.g. *m/z* 41, 55, 69). However, the total organic aerosol mass spectra from oil *versus* food in oil are similar (Pearson's correlation coefficient, *r* = 0.97). Furthermore, separating the mass spectrum into the C_xH_y⁺ and C_xH_yO_z⁺ ion families results in correlation coefficients of 0.99 and 0.94, respectively. The high correlation indicates that the mass spectral signature of the stir fry cooking aerosol is dominated by the contribution of cooking oil to the aerosol.

Tracer ion ratios provide additional insight into the COA chemistry. The abundance of COA is often indicated by a ratio of the signals at *m/z* 55 : 57 > 1, but other ion ratios such as *m/z* 41 : 43 may also differentiate COA by cooking method or meal.^{70,73} We found the 55 : 57 ratio to be 2.26 for the oil splash and 1.80 for the stir fry. These ratios are consistent with the 1.5–4 range observed during outdoor ambient and primary source studies.^{70,72,74,75} The relative difference between the oil splash and stir-fry mass spectra (Fig. 7e) contains strong negative C_xH_yO_z⁺ peaks at *m/z* 44, 60, and 73, indicating that these oxidized ions are emitted from the food ingredients, *i.e.* the vegetables and/or sauce.

Cooking is clearly an important aerosol source indoors, and has also been observed to be an important aerosol component outdoors in urban environments.^{72,76} These initial mass spectral comparisons from HOMEChem reinforce previous source studies⁷⁰ and highlight the challenge in defining COA with one mass spectral ratio or factor. Outdoor COA is difficult to separate from hydrocarbon organic aerosol (HOA) due to the predominance of C_xH_y⁺ ions and spectral similarity between the two components.⁷² Preliminary analysis of the HOMEChem data suggests that specific ratios within the C_xH_y⁺ and C_xH_yO_z⁺ families may help differentiate these otherwise similar spectra in future studies.

3.3 Case study 3: VOC sources

The comprehensive suite of instruments enables a detailed characterization of indoor VOCs at HOMEChem. It is clear from

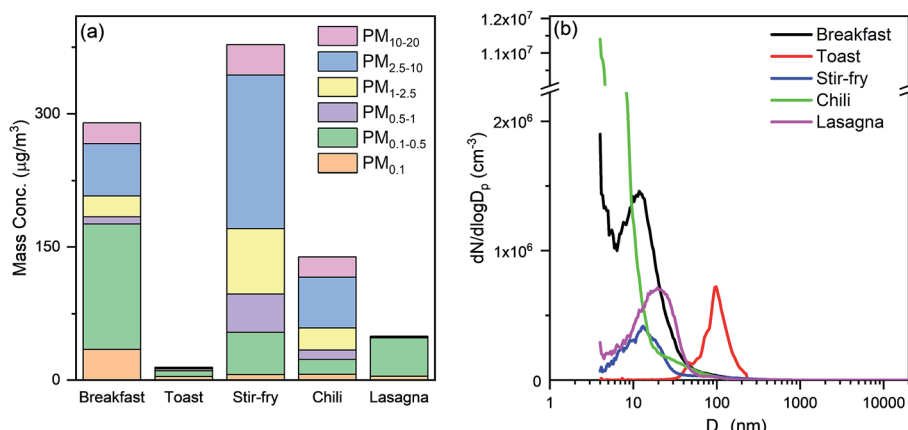


Fig. 6 (a) The highest mass concentrations by size (PM_{0.1}, PM_{0.5}, PM₁, PM_{2.5}, PM₁₀, and PM₂₀) during the preparation of each meal. (b) Particle number size distributions (electrical mobility size: 4 nm–532 nm; aerodynamic size: 542 nm–19.8 µm) corresponding to the highest PM mass concentrations recorded during different types of meals cooked. Mass calculations from size distribution measurements assume a constant aerosol density of 1 g cm⁻³.



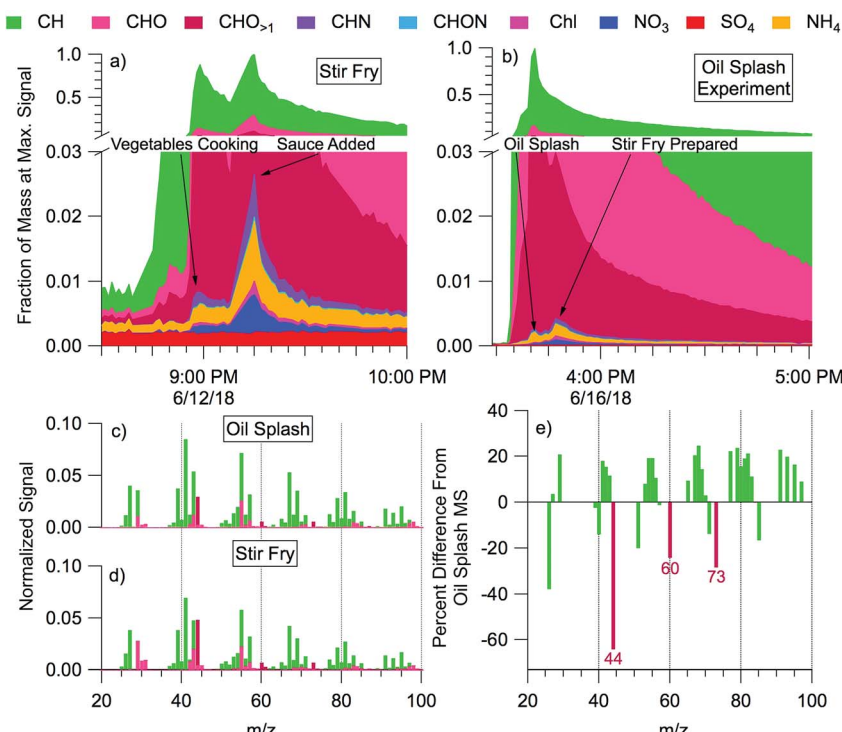


Fig. 7 Time series of non-refractory submicron aerosol composition from (a) cooking stir-fry and (b) aerosolized oil during an oil splash. Stacked times series of species detected by the HR-AMS are scaled to the maximum concentration of each event for comparison, with key activities labeled. Normalized organic mass spectra for (c) oil splash and (d) stir-fry experiments show the $C_xH_y^+$ ions in green and $C_xH_yO_z^+$ ions in magenta. The normalized signal represents each ion family's fractional contribution to total aerosol mass scaled to the maximum concentration observed during the given experiment. The stir fry aerosol mass spectrum (d) is an average of normalized mass spectra calculated over the duration of each stir fry cooking event ($n = 12$), while the oil splash mass spectrum (c) is a 15 minute average taken after pure oil was heated and aerosolized by droplets of water added to the pan ($n = 1$). Frame (e) shows the percent difference oil splash versus stir-fry mass spectra [(oil MS – stir fry MS)/oil MS $\times 100\%$]. Aerosol mass is calculated as a normalized nitrate equivalent mass (i.e. assuming all masses have ionization efficiencies equal to nitrate in the HR-AMS; RIE = 1.0).

preliminary analyses that the sources and behavior of some VOCs, including the oxidized organic acids, are complex. Certain emission sources, such as cleaning product use and human metabolism, have expected effects on indoor VOCs. These features are well illustrated during the layered experiment days (Fig. 8). The gas stove was used three times throughout the day (breakfast, lunch, dinner), resulting in increases in NO, NO₂, CO₂, and ethyne (acetylene). (The gas stove used propane, and concentrations of this species varied substantially across layered days, suggesting a small fuel leak, possibly from the pilot light.) Ozone is consistently low (~ 5 ppb), but the measurement signal rises slightly during bleach mopping events, possibly due to an interference. Mopping with pine-scented cleaner raised limonene levels, while mopping with bleach solution raised chloroform levels. Both isoprene and acetone are known human metabolic emissions, and concentrations of both species were elevated throughout each layered day. Isoprene shows a rapid drop after each bleach mopping event, consistent with consumption by chemical reactions. We note that the chemical signatures are consistent across the layered days despite the variability of outdoor conditions and expected internal variability in volunteer behavior, demonstrating the replicability of the HOMEChem

experimental data (Fig. S7†). Concentrations of most VOCs and trace gases are similar during the same events on different days. For example, CHCl₃ reaches a concentration maximum at the same time during bleach cleaning and at similar levels (1.23, 1.37 and 1.33 ppb). In contrast, while isoprene reaches similar maxima on the three days, the maximum concentration on the first layered day occurs during lunch cooking, while the maximum on the third layered day occurs during dinner.

VOC observations on the variable occupancy days highlight the role of human sources. Metabolic sources of acetone correlate with the number of occupants, while monoterpenes and D5-siloxanes are likely emissions from personal care products (Fig. 3).

While hydrocarbons like limonene, propane, and isoprene varied following their expected cooking, cleaning and human emissions, the time series of organic acids displayed evidence of more complex sources and sinks. Organic acids are prominent in the outdoor atmosphere,^{30,77,78} but also have indoor sources, including human metabolism, building materials, and oxidation chemistry.⁷⁹⁻⁸¹ Exchange of indoor and outdoor air means that outdoor sources may contribute to indoor air organic acid concentrations. Fig. 9 shows indoor and outdoor measurements of various gas phase organic acids during a lengthy background

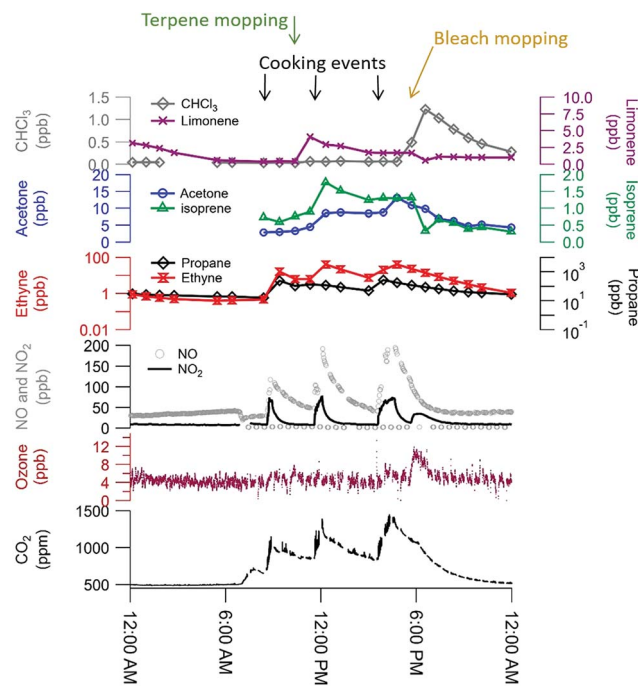


Fig. 8 Trace gas data during a layered experiment day highlights influences of human occupancy, cooking, and cleaning perturbations. Researchers entered the house 7–7:30 am for instrument maintenance and preparation, accounting for the initial rise in CO_2 (exhaled human breath) and drop in NO_x (door opening brings in outdoor air). Three occupants remained in the house from 8:25 am through 5:45 pm (detailed schedule in ESI Section 6).†

period from HOMEChem using iodide CIMS. No in-house experiments were performed during this period and occupancy was minimal, allowing us to explore indoor sources of these compounds from the building and its static contents. Indoor formic and acetic acid mixing ratios remain relatively stable throughout the background period, with an average indoor mixing ratio for formic acid of 30 ppb and acetic acid of 22 ppb. Both organic acids rapidly fluctuate $\pm 10\%$ around their mean mixing ratios in relation to HVAC cycling. These mixing ratios are comparable to levels previously reported in homes during summer. For example, Reiss *et al.*⁷⁹ observed 8–33 ppb of formic and 9–88 ppb of acetic acid; Duncan *et al.*⁸¹ observed 10–30 ppb of formic and 10–40 ppb of acetic acid.

Indoor sources of formic and acetic acid during unoccupied, unperturbed background periods include off-gassing from building materials and household products^{79,82} and O_3 -initiated reactions.^{79,83} As in earlier studies, our data show higher concentrations of formic and acetic acids indoors than outdoors, demonstrating the importance of indoor sources. Outdoor concentrations have little effect on indoor formic and acetic acid. In contrast to indoors, outdoor formic and acetic acid exhibit strong diel patterns during the study, consistent with previous outdoor measurements that indicate photochemical sources of these acids.^{77,78,84} The high ($\gg 1$) indoor/outdoor concentration ratios for formic and acetic acid are consistent with the interior of the HOMEChem building being a non-photochemical source of these two acids to the

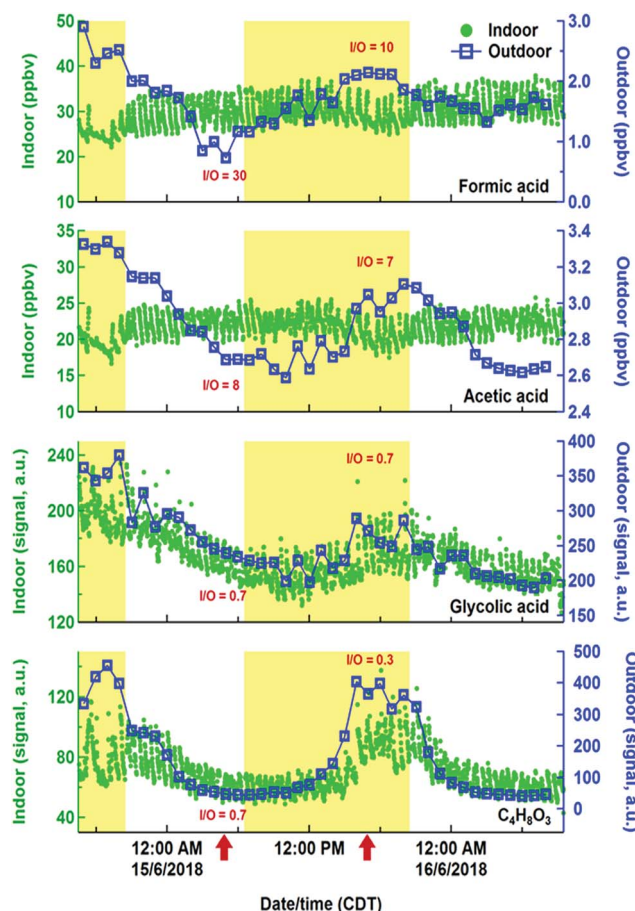


Fig. 9 Time series of indoor (green markers) and outdoor (blue lines and markers) iodide CIMS measurements of formic acid, acetic acid, glycolic acid, and $\text{C}_4\text{H}_8\text{O}_3$ during an extensive background period. Formic and acetic acid data are calculated concentrations (part per billion by volume). Glycolic acid and $\text{C}_4\text{H}_8\text{O}_3$ data are measured CIMS signal (arbitrary units). Red arrows indicate approximate times during which representative indoor-to-outdoor ratios (I/O) are evaluated (June 15 at approximately 04:30 and 16:30). Daytime (06:30–20:30) periods are indicated by yellow highlighted regions.

atmosphere. Assuming these acids are in steady state with indoor surfaces, we estimate an upper bound emission rate from indoors to outdoors to be $2 \times 10^{-4} \text{ mol h}^{-1}$ for formic acid and $1 \times 10^{-4} \text{ mol h}^{-1}$ for acetic acid. This calculation assumes indoor-to-outdoor transport was 100% efficient, although water soluble oxygenated VOCs can be lost to indoor surfaces.⁸¹ A test house-equivalent area of managed lawn soil would be expected to emit $\sim 6 \times 10^{-5} \text{ mol h}^{-1}$ of formic acid and $3\text{--}5 \times 10^{-4} \text{ mol h}^{-1}$ of acetic acid.⁸⁵ Residential homes may therefore be a stronger source of formic acid to outdoor urban atmospheres than area-equivalent emissions from soil.

The building is apparently not a source of all organic acids to the outdoor atmosphere during HOMEChem. The indoor to outdoor ratio of glycolic acid and $\text{C}_4\text{H}_8\text{O}_3$ (likely hydroxybutyric acid) are less than 1 (Fig. 9), consistent with an outdoor source contributing substantially to the indoor abundance. Both the outdoor and indoor diel cycles of these two acids maximize in the mid-afternoon, similar to that of O_3 . While the indoor-to-



outdoor ratio for glycolic acid is constant through the day, ratios for $C_4H_8O_3$ are suppressed during the day relative to night. This diel variation implies additional daytime sinks of $C_4H_8O_3$.

The building is a source of many organic acids, but HOMEChem activities highlight a complex array of possible indoor organic acid sources. Similar to previous observations,⁸¹ all water soluble organic acids cycled rapidly throughout the day coincident with the cycling of the HVAC system, and consistent with a hypothesis that the acids are lost to condensing water on the cooling system coils with re-evaporation occurring between cooling cycles. However, a 4 day time series (June 22–25; Fig. 10) for three selected organic acids indicates additional sources and sinks. Sorbic (2,4-hexadienoic acid, $C_6H_8O_2$), lactic (2-hydroxypropanoic acid, $CH_3CHOHCOOH$) and benzoic (benzene carboxylic acid, C_6H_5COOH) acid were all detected by acetate CIMS. Lactic acid has both cooking (e.g. meat cooking for dinner on June 25) and human sources (e.g. increase during open house and maintenance days, June 22 and 23). Benzoic acid has only cooking sources (e.g. cooking lunch on June 25), consistent with its use as a food preservative. Sorbic acid displays a more complex pattern. It is a food preservative and an ingredient in personal care products and cosmetics, and shows clear enhancements during cooking events on the layered day, June 25 (Fig. 10). Personal care products correspond to elevated sorbic acid on the Open House day (June 22), but not on the staggered occupancy day (June 24), which experienced fewer individuals in the house (e.g. a maximum of 12 *versus* 40+ individuals present during the Open House). We observe a decline in sorbic acid mixing ratio throughout the open house day, consistent with its possible presence in personal care

products applied in the morning with diminishing signals as the day progresses, as has been previously reported for the siloxane, D5, widely used in antiperspirants.⁷

Relative to other unoccupied evenings (e.g. night of June 22 or 26), all three acids (sorbic, lactic, and benzoic) were present at elevated concentrations on the night of June 24–25. Although this elevated acid signal coincided with O_3 addition experiments, we speculate that the increased signals are more likely due to higher temperatures in the house that enable shifts in partitioning from indoor surfaces and aerosol particles to indoor air. However, we observed additional increase of sorbic acid signal that overlaps with the O_3 addition periods (indicated by the red arrows in Fig. 10), suggesting that sorbic acid may be an indoor ozonolysis reaction product and that secondary chemistry influences indoor organic acid concentrations – but only under elevated ozone conditions.

3.4 Case study 4: deposition on indoor surfaces

Surfaces play important roles in the lifetime and reactivity of indoor pollutant emissions.^{13,86,87} Trace gases and particles can deposit to surfaces, potentially persisting for extended periods if unperturbed.⁸⁸ Surface deposited material can undergo reactions on much longer timescales than indoor air reactions, which are typically limited to hours by the time scale of building air exchange. Organic films on surfaces can also alter chemical and physical properties at the air-surface interface.^{89,90} Surface samples were collected during HOMEChem, and here we describe initial results aimed at understanding the chemical, physical and morphological state of surface-bound species.

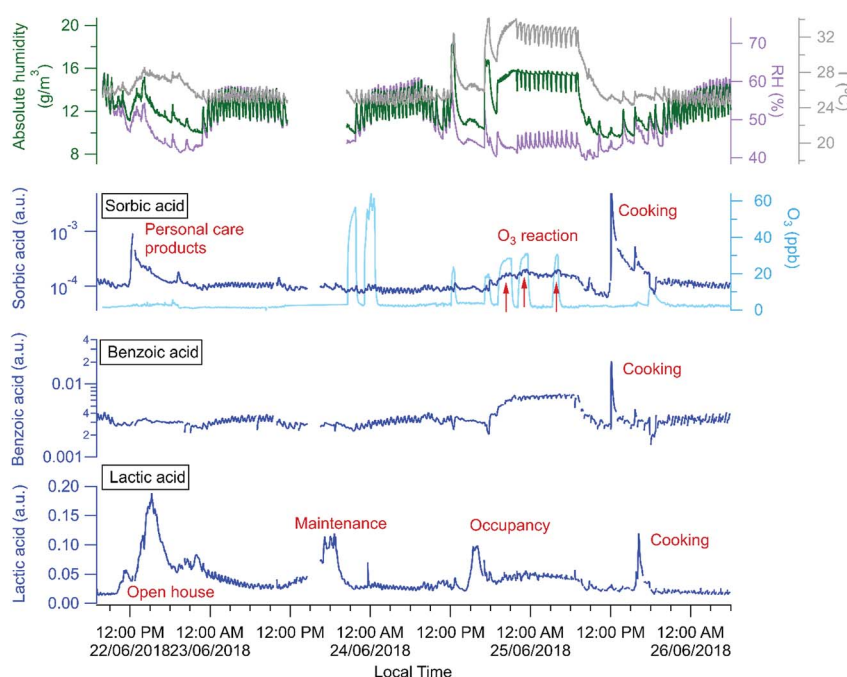


Fig. 10 Three organic acids – sorbic, benzoic, and lactic acid – varied during four days of the campaign (open house, maintenance, occupancy, and layered day) with temperature in grey, relative humidity/RH in purple, and absolute humidity/AH in dark green. Cooking or food sources of all three organic acids are apparent, as are occupant emissions of lactic acid and personal care product sources of sorbic acid.



Deposited particles were collected on vertically-mounted pieces of window glass. Analyses are presented in detail in ESI Section S2.† As expected, the surfaces collected more particles across the entire submicron size range during stir-fry events (equivalent average film growth rate of $0.09 \pm 0.05 \text{ nm h}^{-1}$, though only a small fraction of the glass surface was covered with particles) compared to unoccupied periods (thickness growth rate of $0.02 \pm 0.03 \text{ nm h}^{-1}$). Consistent with measured aerosol size distributions, many deposited particles were ultrafine ($<100 \text{ nm}$), with a peak in the number *versus* volume equivalent diameter at approximately 20 nm in diameter (Fig. S8†). The predominance of ultrafine particle deposition on window glass is consistent with previous studies of kitchen activities.^{91–93}

We probed the surface-bound particles with atomic force microscopy coupled to infrared imaging (AFM-IR). Fig. 11 shows the 3-D height image and line profile for a single particle deposited on window glass from a stir-fry event along with the infrared spectra collected across the particle at the corresponding marked location. These spectral features suggest that the particle is largely comprised of carboxylate containing organics, as shown by the peaks at around 1570 and 1430 cm^{-1} associated with the asymmetric (ν_{as}) and symmetric (ν_{s}) stretching vibration modes for carboxylate.⁹⁴ The detection of carboxylate groups is consistent with deposition of fatty acids emitted during the stir fry process⁹¹ – and with the aerosol mass spectra discussed in the cooking case study (§3.2). The absence of the vibrational mode at 1700 cm^{-1} associated with the $\text{C}=\text{O}$ stretch for protonated carboxylic acid groups suggests either deprotonation of the fatty acid-rich particles *via* binding between the carboxylate group with the silica and metal ions from the window glass, or that the surface film is alkaline in nature leading to the presence of deprotonated carboxylate groups.

Surface depositions were also extracted from multiple glass surfaces and analyzed for bulk composition using an array of techniques. In contrast to previous longer-term studies of glass exposed for 3 to 6 months,⁸⁸ inductively-coupled plasma mass spectrometry (ICP-MS) detected little difference in elemental composition of surface depositions from the unoccupied background, cooking (shakedown day), and stir-fry samples. Compared to the unoccupied background, only iron and magnesium showed significant enrichment in the shakedown

(50% increase) and stir-fry sample (31% increase), respectively (Fig. S9 and Table S1†). The lack of differentiation in surface deposition of metals suggests relatively low levels of metal emissions during cooking, in addition to smaller sample size and decreased exposure durations in comparison to previous work. Relatively high background levels are attributable to metals in window glass leaching into the extraction solvent.

The similarity between organic molecules accumulated on surfaces and the lower volatility material present in aerosol particles is apparent from a direct comparison of deposited material and indoor and outdoor aerosol samples. In a separate set of samples from the ones discussed above, two large glass surfaces were mounted vertically above the stove for the duration of the campaign. Solvent extractions utilized a custom-built indoor surface extractor with acetonitrile. In addition to the surface samples, two different filters collected aerosol particles indoors and outdoors for the duration of the campaign, and were also extracted by acetonitrile solvent. The chemical composition of the water soluble fraction of these surface and aerosol filter extracts was analyzed by HR-AMS following atomization by a Small Volume Nebulizer.⁵⁰ This analysis approach enables a comparison of ensemble properties of the organic material on surfaces and in aerosol particles.

The signal intensities of the mass spectra for the indoor aerosol filter and surface extracts have high overlap, with a dot product of 0.98 (Fig. 12a). In contrast, mass spectra of surface extracts and outdoor aerosol show less overlap (dot product of 0.86, Fig. 12b). The similar chemical composition between the indoor aerosol filter and the organic matter deposited near the stove indicates that indoor generated aerosol is the dominant source of these surface deposits. The indoor aerosol is less oxidized than the outdoor sample, with an average O/C of 0.21 indoors *versus* 0.30 outdoors. The outdoor aerosol sample also has more nitrogen containing organic ions compared to the indoor aerosol and surface samples. Differences between the campaign-averaged surface extracts and indoor aerosol are small, with slightly lower H/C ratios on the surface. The examples presented in this case study demonstrate advances in analytical techniques to better understand the chemical and physical properties of material deposited on indoor surfaces.

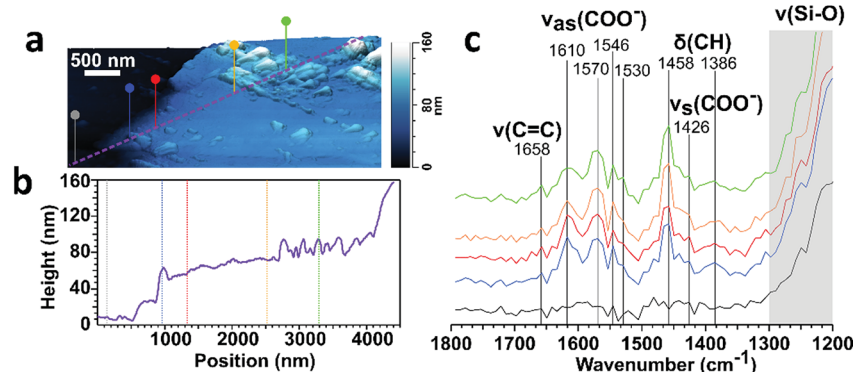


Fig. 11 (a) 3-D AFM height image of a deposition on window glass from a stir-fry event. (b) Height profile from the purple line shown in panel (a). (c) IR spectra taken at the corresponding colored markers in panels A and B.

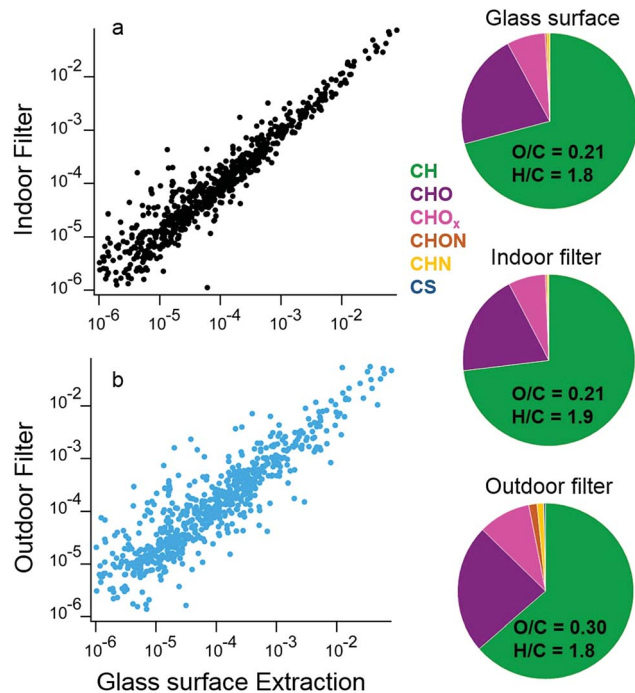


Fig. 12 Off-line AMS measurements of extracts from filters sampling indoors and outdoors for the full campaign are compared to extracted surface depositions from a glass surface deployed above the stove during the campaign. The intensities of each peak in the mass spectra are compared for surface extracts and (a) the indoor aerosol filter or (b) the outdoor aerosol filter. The pie charts on the right show the mass fractions of different ion types for the glass surface, indoor aerosol filter, and outdoor aerosol filter.

3.5 Case study 5: intercomparison of NO₂ measurements

The HOMEChem study design intentionally measured the same gas and particle analytes by multiple instruments (Tables 1–4). This approach not only ensured data coverage in the event of instrument problems, but also provided opportunities for measurement intercomparisons in the indoor environment. Several observations were as expected. For example, ultrafine particles initially provided spurious signal in the UV absorption O₃ detector,⁹⁵ but filters placed on inlets minimized this interference. Nitrogen dioxide provides a useful case study for instrument intercomparisons: despite their prevalence in air pollution monitoring, the outdoor atmospheric chemistry community has long noted interferences in some of the most commonly used NO₂ detection techniques.⁵⁸ Here, we compare NO₂ detected indirectly by the blue light converter coupled to chemiluminescence NO detection (hereafter BLC-NO₂) compared to NO₂ detected directly by cavity attenuated phase-shift spectroscopy (CAPS) (hereafter CAPS-NO₂). The BLC and CAPS detector inlets were located adjacent to each other. Differences in time averaging – namely the slower time resolution of the BLC detector – account for some of the suppressed BLC-NO₂ measurements during rapid events. However, even accounting for these distinctions, discrepancies between the two measurement systems persist.

During intensive cooking events, BLC-NO₂ provides strong negative readings – as low as –853 ppb during the Thanksgiving

event of 18 June. We attribute these negative values for BLC-NO₂ to VOC interferences in the photolysis cell. Molecules like glyoxal can produce HO₂ upon photolysis by blue light that converts NO to NO₂. The resulting HO₂ suppresses the NO in the detected NO + NO₂ total from the blue light converter, resulting in a NO_x signal that is smaller than NO, and thus a negative NO₂ if ambient NO is greater than ambient NO₂. The HOMEChem Thanksgiving observations are consistent with this inferred interference: at 15:45 on 18 June, NO is 965 ppb, while NO₂ is reported as –853 ppb (Fig. 13c). Thus, there is enough RO₂ or HO₂ formed within the blue light converter to transform almost all of the NO to NO₂ and outcompete simultaneous NO₂ photolysis. The result is only 112 ppb NO entering the chemiluminescence detector from the blue light converter during NO_x detection mode. The negative BLC-NO₂ implies that substantial RO₂-producing (*i.e.* photolabile) VOCs are present indoors during the Thanksgiving experiments. This observation is consistent with elevated levels of organic molecules including peroxide, carboxylic acid and carbonyl moieties. If such photolabile molecules move from indoor air to the outdoor atmosphere, they may contribute to urban outdoor radical budgets.

In addition to Thanksgiving, BLC-NO₂ was also negative at the end of each layered day when NO_x was elevated above background from cooking and volunteers mopped with bleach before exiting the test house. This negative BLC-NO₂ suggests that chlorine chemistry is a source of radicals that react with NO_x under blue light, potentially through the production of HO₂ or RO₂ radicals.

During sequential chlorine bleach mopping, the CAPS-NO₂ signal increased above background concentrations, while the BLC-NO₂ remained stable or even slightly suppressed. These simultaneous yet opposite trends in CAPS-NO₂ and BLC-NO₂ occurred in the absence of NO_x addition from cooking on both sequential bleach mopping days (7 and 10 June) (Fig. 13b). These intercomparison deviations may be the result of a negative interference in BLC-NO₂ from NO reactions in the photolytic converter, or possibly a positive interference in CAPS-NO₂ from chlorinated species.

The BLC detector consistently detects higher background of unperturbed NO₂ inside the house than the CAPS detector (Fig. 13a). This systematic difference may be due to different background and calibration approaches between the two systems. Removing all data points in which the relative error of BLC-NO₂ ($\sigma_{\text{BLC NO}_2}/[\text{NO}_2] \times 100\%$) is below 0 or above 50% identifies the cooking interferences described above. However, once these points are removed, we still observe a persistent bias causing CAPS-NO₂ to be higher than BLC-NO₂ ($r^2 = 0.69$, slope 2.16 ± 0.01), even when chlorine bleach cleaning events are removed. The histogram of the difference between CAPS-NO₂ and BLC-NO₂ follows a Gaussian distribution with a mean difference of 0.6 ppb and a standard deviation of 1.3 ppb, consistent with an offset in the instrument calibrations and background. However, restricting the analysis further to unperturbed house conditions only (*i.e.* when CAPS-NO₂ < 10 ppb and BLC-NO₂ > 0 ppb) results in a slope of 0.99 ± 0.01 . Thus, the two instruments agree well under low-NO₂, unperturbed conditions. Under these unperturbed, low-NO_x conditions, the correlation coefficient between the two timeseries



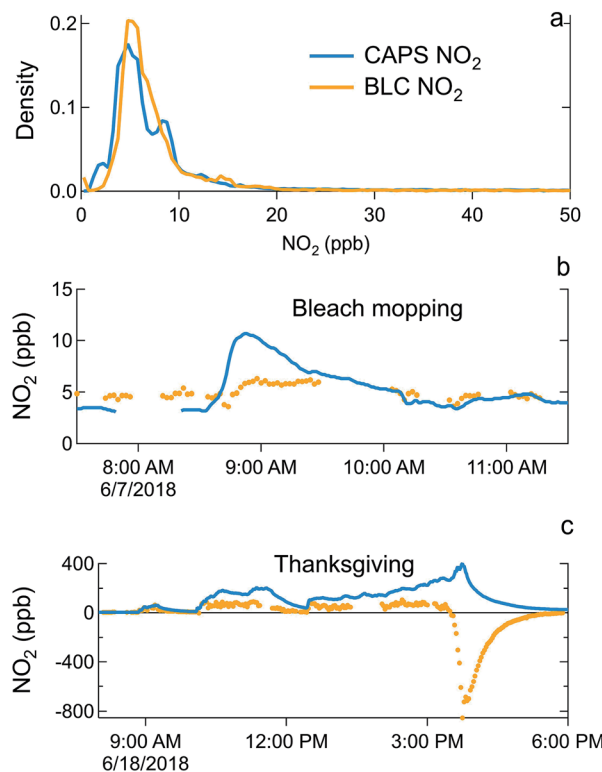


Fig. 13 Normalized probability distributions of background indoor NO₂ (a) demonstrates that NO₂ detected by the CAPS (CAPS-NO₂, blue) is slightly lower than the blue-light converter (BLC-NO₂, orange). (b) CAPS-NO₂ is enhanced during bleach mopping events, while BLC-NO₂ does not change substantially during bleach mopping. (c) BLC-NO₂ is subject to negative interferences during intensive cooking events, including Thanksgiving. Breaks in the BLC-NO₂ timeseries occur when the sampling manifold switched to outdoor air (excluded from this figure).

is low (r^2 of 0.55), but this outcome may be due to limits on the relative precision of the instruments. This instrument intercomparison highlights the need for overlapping measurements of even commercially available or simpler instrumentation, particularly when intended for use in indoor environments.

4. Conclusions

The HOMEChem field campaign represents coordinated deployment of a particularly large assemblage of indoor air and surface measurement capabilities applied to simulated real-life conditions in a full-sized test house. The case studies described here illustrate several aspects of human influence on trace gas and particle composition of residential air through direct emissions, use of commercial products, and occupant activities. The research has focused on everyday activities performed in home environments (*i.e.* cooking, cleaning, and human occupancy). The study also offers the opportunity to contrast indoor and outdoor background air in a residential test house.

Background air is generally lower in particle concentration indoors than outdoors. During cooking events, large enhancements in particle mass occur, with a substantial fraction of

these increases due to chemical species related to cooking oils. By number, these cooking-associated particles are predominantly in the ultrafine mode, but substantial mass changes are observed in the accumulation and super-micron modes. The emitted particles remain in indoor air for short periods relative to persistence time scales in the outdoor atmosphere. Indoor emitted particles also evolve chemically throughout the cooking processes, with particles becoming slightly more oxygenated and nitrogenated when food is added to cooking oil. The chemical signature of cooking aerosol is observed in the organic molecules deposited on surfaces, as evidenced through both mass spectrometry and spectroscopic techniques. The large amount of organic material deposited on indoor surfaces can interact with the surface itself, as evidenced by the AFM-IR results.

Cooking also generates gas phase emissions, including hydrocarbons and more complex oxidized organic molecules, such as sorbic and lactic acid. Even in the absence of cooking or other perturbations, gas phase organics were generally higher indoors than outdoors across a broad range of species. Indoor concentrations of formic and acetic acid during HOMEChem were consistent with levels reported in previous studies. Persistently high concentrations of organic acids indoors suggest that buildings themselves may be sources of these compounds to outdoor air.

HOMEChem highlights the opportunities for new measurement techniques, including real-time high resolution time-of-flight mass spectrometry and surface measurements, for investigating the complex influences of buildings, occupants, and their activities on indoor chemistry. The instrument intercomparisons also highlight some new challenges in indoor chemistry research: the vast array of previously unmeasured and unexpected compounds that are clearly present indoors can complicate measurements and thus interpretation of chemical data. The HOMEChem dataset is, in itself, a promising demonstration of the usefulness of open-access experimental data to the indoor air quality community as well-curated and archived datasets can be used by researchers from a variety of fields, such as chemists, engineers, exposure scientists, and toxicologists to model chemical reactions, estimate exposure levels, and develop appropriate risk management strategies, among many other possibilities.

Data availability

All final data from the HOMEChem project will be available in the ICARTT format to other researchers within two years of the conclusion of the field measurements (*i.e.* by July 1, 2020).

Conflicts of interest

There are no conflicts to declare.

Acknowledgements

We thank the entire HOMEChem science team of faculty, researchers, and students, over 60 members in total, for



operating instruments, volunteering for activities, and contributing to experimental design. We thank the Alfred P. Sloan Foundation for funding the HOMEChem experiment and analysis (G-2017-9944; G-2017-9692; G-2016-7049; G-2016-7050, G-2018-11062; G-2018-11031; G-2018-10128; G-2018-11366; G-2018-11035, G-2016-7173). JLJ also acknowledges funding from the CIRES Innovative Research Program. Dr Manabu Shiraiwa, Dr Glenn Morrison and the MOCCIE group provided input on experimental design. We acknowledge the Novoselac research group for preparing and operating the test house, the UT Austin CEER staff for logistical support, and the UT Austin Pickle Research Campus for hosting the research project. REO thanks Jesse H. Kroll at MIT for the use of his HR-ToF-AMS for off-line AMS data collection.

References

- 1 N. E. Klepeis, W. C. Nelson, W. R. Ott, J. P. Robinson, A. M. Tsang, P. Switzer, J. V. Behar, S. C. Hern and W. H. Engelmann, The National Human Activity Pattern Survey (NHAPS): A resource for assessing exposure to environmental pollutants, *J. Exposure Anal. Environ. Epidemiol.*, 2001, **11**, 231–252.
- 2 K. Koehler, N. Good, A. Wilson, A. Mölter, B. F. Moore, T. Carpenter, J. L. Peel and J. Volckens, The Fort Collins commuter study: Variability in personal exposure to air pollutants by microenvironment, *Indoor Air*, 2019, **29**, 231–241.
- 3 D. Campagnolo, D. E. Saraga, A. Cattaneo, A. Spinazze, C. Mandin, R. Mabilia, E. Perreca, I. Sakellaris, N. Canha, V. G. Mihucz, T. Szigeti, G. Ventura, J. Madureira, E. D. Fernandes, Y. de Kluizenaar, E. Cornelissen, O. Hanninen, P. Carrer, P. Wolkoff, D. M. Cavallo and J. G. Bartzis, VOCs and aldehydes source identification in European office buildings - The OFFICAIR study, *Building and Environment*, 2017, **115**, 18–24.
- 4 Y. Liu, P. K. Misztal, J. Xiong, Y. Tian, C. Arata, R. J. Weber, W. W. Nazaroff and A. H. Goldstein, Characterizing sources and emissions of volatile organic compounds in a northern California residence using space-and time-resolved measurements, *Indoor Air*, 2019, **29**(4), 630–644, DOI: 10.1111/ina.12562.
- 5 J. P. S. Wong, N. Carslaw, R. Zhao, S. Zhou and J. P. D. Abbatt, Observations and impacts of bleach washing on indoor chlorine chemistry, *Indoor Air*, 2017, **27**, 1082–1090.
- 6 A. C. Steinemann, I. C. MacGregor, S. M. Gordon, L. G. Gallagher, A. L. Davis, D. S. Ribeiro and L. A. Wallace, Fragrance consumer products: Chemicals emitted, ingredients unlisted, *Environmental Impact Assessment Review*, 2011, **31**, 328–333.
- 7 X. Tang, P. K. Misztal, W. W. Nazaroff and A. H. Goldstein, Siloxanes are the most abundant volatile organic compound emitted from engineering students in a classroom, *Environ. Sci. Technol. Lett.*, 2015, **2**, 303–307.
- 8 P. K. Misztal, D. S. Lymeropoulou, R. I. Adams, R. A. Scott, S. E. Lindow, T. Bruns, J. W. Taylor, J. Uehling, G. Bonito, R. Vilgalys and A. H. Goldstein, Emission factors of microbial volatile organic compounds from environmental bacteria and fungi, *Environ. Sci. Technol.*, 2018, **52**, 8272–8282.
- 9 J. Williams, C. Stönnér, J. Wicker, N. Krauter, B. Derstroff, E. Bourtsoukidis, T. Klüpfel and S. Kramer, Cinema audiences reproducibly vary the chemical composition of air during films, by broadcasting scene specific emissions on breath, *Sci. Rep.*, 2016, **6**, 25464.
- 10 L. A. Wallace, S. J. Emmerich and C. Howard-Reed, Source strengths of ultrafine and fine particles due to cooking with a gas stove, *Environ. Sci. Technol.*, 2004, **38**(8), 2304–2311.
- 11 K. Kristensen, D. M. Lunderberg, Y. Liu, P. K. Misztal, Y. Tian, C. Arata, W. W. Nazaroff and A. H. Goldstein, Sources and dynamics of semivolatile organic compounds in a single-family residence in Northern California, *Indoor Air*, 2019, **29**(4), 645–655, DOI: 10.1111/ina.12561.
- 12 G. Morrison, Interfacial chemistry in indoor environments, *Environ. Sci. Technol.*, 2008, **42**, 3494–3499.
- 13 C. J. Weschler and N. Carslaw, Indoor chemistry, *Environ. Sci. Technol.*, 2018, **52**, 2419–2428.
- 14 N. Carslaw, A new detailed chemical model for indoor air pollution, *Atmos. Environ.*, 2007, **41**, 1164–1179.
- 15 M. M. Coggon, B. C. McDonald, A. Vlasenko, P. R. Veres, F. Bernard, A. R. Koss, B. Yuan, J. B. Gilman, J. Peischl, K. C. Aikin, J. DuRant, C. Warneke, S. M. Li and J. A. de Gouw, Diurnal variability and emission pattern of decamethylcyclopentasiloxane (D-5) from the application of personal care products in two North American cities, *Environ. Sci. Technol.*, 2018, **52**, 5610–5618.
- 16 B. C. McDonald, J. A. de Gouw, J. B. Gilman, S. H. Jathar, A. Akherati, C. D. Cappa, J. L. Jimenez, J. Lee-Taylor, P. L. Hayes, S. A. McKeen, Y. Y. Cui, S. W. Kim, D. R. Gentner, G. Isaacman-VanWertz, A. H. Goldstein, R. A. Harley, G. J. Frost, J. M. Roberts, T. B. Ryerson and M. Trainer, Volatile chemical products emerging as largest petrochemical source of urban organic emissions, *Science*, 2018, **359**, 760–764.
- 17 D. K. Farmer and J. L. Jimenez, Real-time atmospheric chemistry field instrumentation, *Anal. Chem.*, 2010, **82**(19), 7879–7884, DOI: 10.1021/ac1010603.
- 18 D. K. Farmer, Analytical challenges and opportunities for indoor air chemistry field studies, *Anal. Chem.*, 2019, **91**, 3761–3767.
- 19 C. Arata, K. J. Zarzana, P. K. Misztal, Y. J. Liu, S. S. Brown, W. W. Nazaroff and A. H. Goldstein, Measurement of NO_3 and N_2O_5 in a Residential Kitchen, *Environ. Sci. Technol. Lett.*, 2018, **5**, 595–599.
- 20 D. B. Collins, R. F. Hems, S. M. Zhou, C. Wang, E. Grignon, M. Alavy, J. A. Siegel and J. P. D. Abbatt, Evidence for gas-surface equilibrium control of indoor nitrous acid, *Environ. Sci. Technol.*, 2018, **52**, 12419–12427.
- 21 S. F. Kowal, S. R. Allen and T. F. Kahan, Wavelength-resolved photon fluxes of indoor light sources: Implications for HOx production, *Environ. Sci. Technol.*, 2017, **51**, 10423–10430.
- 22 A. M. Avery, M. S. Waring and P. F. DeCarlo, Human occupant contribution to secondary aerosol mass in the



indoor environment, *Environ. Sci.: Processes Impacts*, 2019, DOI: 10.1039/C9EM00097F.

23 P. F. DeCarlo, A. M. Avery and M. S. Waring, Thirdhand smoke uptake to aerosol particles in the indoor environment, *Sci. Adv.*, 2018, **4**, eaap8368, DOI: 10.1126/sciadv.aap8368.

24 P. L. Kebabian, E. C. Wood, S. C. Herndon and A. Freedman, A practical alternative to chemiluminescence-based detection of nitrogen dioxide: Cavity attenuated phase shift spectroscopy, *Environ. Sci. Technol.*, 2008, **42**, 6040–6045.

25 S. Dusanter, D. Vimal and P. S. Stevens, Technical note: Measuring tropospheric OH and HO₂ by laser-induced fluorescence at low pressure. A comparison of calibration techniques, *Atmos. Chem. Phys.*, 2008, **8**, 321–340.

26 S. Dusanter, D. Vimal, P. S. Stevens, R. Volkamer, L. T. Molina, A. Baker, S. Meinardi, D. Blake, P. Sheehy, A. Merten, R. Zhang, J. Zheng, E. C. Fortner, W. Junkermann, M. Dubey, T. Rahn, B. Eichinger, P. Lewandowski, J. Prueger and H. Holder, Measurements of OH and HO₂ concentrations during the MCMA-2006 field campaign - Part 2: Model comparison and radical budget, *Atmos. Chem. Phys.*, 2009, **9**, 6655–6675.

27 M. M. Lew, S. Dusanter and P. S. Stevens, Measurement of interferences associated with the detection of the hydroperoxy radical in the atmosphere using laser-induced fluorescence, *Atmos. Meas. Tech.*, 2018, **11**, 95–109.

28 A. Abeleira, I. B. Pollack, B. Sive, Y. Zhou, E. V. Fischer and D. K. Farmer, Source characterization of volatile organic compounds in the Colorado Northern Front Range Metropolitan Area during spring and summer 2015, *J. Geophys. Res.: Atmos.*, 2017, **122**, 3595–3613.

29 X. Tang, P. K. Misztal, W. W. Nazaroff and A. H. Goldstein, Volatile organic compound emissions from humans indoors, *Environ. Sci. Technol.*, 2016, **50**, 12686–12694.

30 P. Brophy and D. K. Farmer, A switchable reagent ion high resolution time-of-flight chemical ionization mass spectrometer for real-time measurement of gas phase oxidized species: characterization from the 2013 southern oxidant and aerosol study, *Atmos. Meas. Tech.*, 2015, **8**, 2945–2959.

31 J. M. Roberts, P. Veres, C. Warneke, J. A. Neuman, R. A. Washenfelder, S. S. Brown, M. Baasandorj, J. B. Burkholder, I. R. Burling, T. J. Johnson, R. J. Yokelson and J. de Gouw, Measurement of HONO, HNCO, and other inorganic acids by negative-ion proton-transfer chemical-ionization mass spectrometry (NI-PT-CIMS): application to biomass burning emissions, *Atmos. Meas. Tech.*, 2010, **3**, 981–990.

32 R. F. Hems, C. Wang, D. B. Collins, S. Zhou, N. Borduas-Dedekind, J. A. Siegel and J. P. D. Abbatt, Sources of isocyanic acid (HNCO) indoors: a focus on cigarette smoke, *Environ. Sci.: Processes Impacts*, 2019, DOI: 10.1039/C9EM00107G.

33 F. D. Lopez-Hilfiker, C. Mohr, M. Ehn, F. Rubach, E. Kleist, J. Wildt, T. F. Mentel, A. Lutz, M. Hallquist, D. Worsnop and J. A. Thornton, A novel method for online analysis of gas and particle composition: description and evaluation of a Filter Inlet for Gases and AEROSols (FIGAERO), *Atmos. Meas. Tech.*, 2014, **7**, 983–1001.

34 G. Isaacman, N. M. Kreisberg, L. D. Yee, D. R. Worton, A. W. H. Chan, J. A. Moss, S. V. Hering and A. H. Goldstein, Online derivatization for hourly measurements of gas- and particle-phase semi-volatile oxygenated organic compounds by thermal desorption aerosol gas chromatography (SV-TAG), *Atmos. Meas. Tech.*, 2014, **7**, 4417–4429.

35 P. F. DeCarlo, J. R. Kimmel, A. Trimborn, M. J. Northway, J. T. Jayne, A. C. Aiken, M. Gonin, K. Fuhrer, T. Horvath, K. S. Docherty, D. R. Worsnop and J. L. Jimenez, Field-deployable, high-resolution, time-of-flight aerosol mass spectrometer, *Anal. Chem.*, 2006, **78**, 8281–8289.

36 R. Fröhlich, M. J. Cubison, J. G. Slowik, N. Bukowiecki, A. S. H. Prévôt, U. Baltensperger, J. Schneider, J. R. Kimmel, M. Gonin, U. Rohner, D. R. Worsnop and J. T. Jayne, The ToF-ACSM: a portable aerosol chemical speciation monitor with TOFMS detection, *Atmos. Meas. Tech.*, 2013, **6**, 3225–3241.

37 N. L. Ng, S. C. Herndon, A. Trimborn, M. R. Canagaratna, P. L. Croteau, T. B. Onasch, D. Sueper, D. R. Worsnop, Q. Zhang, Y. L. Sun and J. T. Jayne, An Aerosol Chemical Speciation Monitor (ACSM) for routine monitoring of the composition and mass concentrations of ambient aerosol, *Aerosol Sci. Technol.*, 2011, **45**, 780–794.

38 J. Cai, B. Yan, J. Ross, D. Zhang, P. L. Kinney, M. S. Perzanowski, K. Jung, R. Miller and S. N. Chillrud, Validation of MicroAeth® as a black carbon monitor for fixed-site measurement and optimization for personal exposure characterization, *Aerosol Air Qual. Res.*, 2014, **14**, 1–9.

39 L. Drinovec, G. Mocnik, P. Zotter, A. S. H. Prévôt, C. Ruckstuhl, E. Coz, M. Rupakheti, J. Sciare, T. Muller, A. Wiedensohler and A. D. A. Hansen, The “dual-spot” Aethalometer: an improved measurement of aerosol black carbon with real-time loading compensation, *Atmos. Meas. Tech.*, 2015, **8**, 1965–1979.

40 P. K. Diwakar and P. Kulkarni, Measurement of elemental concentration of aerosols using spark emission spectroscopy, *J. Anal. At. Spectrom.*, 2012, **27**, 1101–1109.

41 J. Kangasluoma, A. Franchin, J. Duplissy, L. Ahonen, F. Korhonen, M. Attoui, J. Mikkilä, K. Lehtipalo, J. Vanhanen, M. Kulmala and T. Petäjä, Operation of the Airmodus A11 nano Condensation Nucleus Counter at various inlet pressures and various operation temperatures, and design of a new inlet system, *Atmos. Meas. Tech.*, 2016, **9**, 2977–2988.

42 R. S. Gao, H. Telg, R. J. McLaughlin, S. J. Ciciora, L. A. Watts, M. S. Richardson, J. P. Schwarz, A. E. Perring, T. D. Thornberry, A. W. Rollins, M. Z. Markovic, T. S. Bates, J. E. Johnson and D. W. Fahey, A light-weight, high-sensitivity particle spectrometer for PM2.5 aerosol measurements, *Aerosol Sci. Technol.*, 2016, **50**, 88–99.

43 Y. Cai, D. C. Montague, W. Mooiweer-Bryan and T. Deshler, Performance characteristics of the ultra high sensitivity aerosol spectrometer for particles between 55 and 800 nm:

Laboratory and field studies, *J. Aerosol Sci.*, 2008, **39**, 759–769.

44 B. T. Chen, Y. S. Cheng and H. C. Yeh, Performance of a TSI aerodynamic particle sizer, *Aerosol Sci. Technol.*, 1985, **4**, 89–97.

45 V. Agranovski, Z. Ristovski, M. Hargreaves, P. J. Blackall and L. Morawska, Real-time measurement of bacterial aerosols with the UVAPS: performance evaluation, *J. Aerosol Sci.*, 2003, **34**, 301–317.

46 I. Protsyuk, A. V. Melnik, L. F. Nothias, L. Rappez, P. Phapale, A. A. Aksenenov, A. Bouslimani, S. Ryazanov, P. C. Dorrestein and T. Alexandrov, 3D molecular cartography using LC-MS facilitated by Optimus and 'ili software, *Nat. Protoc.*, 2018, **13**, 134–154.

47 A. P. Ranney and P. J. Ziemann, Microscale spectrophotometric methods for quantification of functional groups in oxidized organic aerosol, *Aerosol Sci. Technol.*, 2016, **50**, 881–892.

48 P. C. Mouli, S. V. Mohan, V. Balaram, M. P. Kumar and S. J. Reddy, A study on trace elemental composition of atmospheric aerosols at a semi-arid urban site using ICP-MS technique, *Atmos. Environ.*, 2006, **40**, 136–146.

49 K. Suzuki, Characterisation of airborne particulates and associated trace metals deposited on tree bark by ICP-OES, ICP-MS, SEM-EDX and laser ablation ICP-MS, *Atmos. Environ.*, 2006, **40**, 2626–2634.

50 R. E. O'Brien, K. J. Ridley, M. R. Canagaratna, J. T. Jayne, P. L. Croteau, D. R. Worsnop, S. H. Budisulistiorini, J. D. Surratt, C. L. Follett, D. J. Repeta and J. H. Kroll, Ultrasonic nebulization for the elemental analysis of microgram-level samples with offline aerosol mass spectrometry, *Atmos. Meas. Tech.*, 2019, **12**, 1659–1671.

51 C. J. Weschler, H. C. Shields and D. V. Naik, Indoor ozone exposures, *JAPCA*, 1989, **39**, 1562–1568.

52 C. J. Weschler, Ozone in indoor environments: Concentration and chemistry, *Indoor Air*, 2000, **10**, 269–288.

53 J. R. Girman, M. G. Apte, G. W. Traynor, J. R. Allen and C. D. Hollowell, Pollutant emission rates from indoor combustion appliances and sidestream cigarette smoke, *Environ. Int.*, 1982, **8**, 213–221.

54 G. W. Traynor, D. W. Anthon and C. D. Hollowell, Technique for determining pollutant emissions from a gas-fired range, *Atmos. Environ.*, 1982, **16**, 2979–2987.

55 G. W. Traynor, J. R. Girman, M. G. Apte, J. F. Dillworth and P. D. White, Indoor air pollution due to emissions from unvented gas-fired space heaters, *J. Air Pollut. Control Assoc.*, 1985, **35**, 231–237.

56 S. S. Park, J. H. Hong, J. H. Lee, Y. J. Kim, S. Y. Cho and S. J. Kim, Investigation of nitrous acid concentration in an indoor environment using an in situ monitoring system, *Atmos. Environ.*, 2008, **42**, 6586–6596.

57 J. E. Borrazzo, J. F. Osborn, R. C. Fortmann, R. L. Keeper and C. I. Davidson, Modeling and monitoring of CO, NO and NO₂ in a modern townhouse, *Atmos. Environ.*, 1987, **21**, 299–311.

58 E. J. Dunlea, S. C. Herndon, D. D. Nelson, R. M. Volkamer, F. San Martini, P. M. Sheehy, M. S. Zahniser, J. H. Shorter, J. C. Wormhoudt, B. K. Lamb, E. J. Allwine, J. S. Gaffney, N. A. Marley, M. Grutter, C. Marquez, S. Blanco, B. Cardenas, A. Retama, C. R. R. Villegas, C. E. Kolb, L. T. Molina and M. J. Molina, Evaluation of nitrogen dioxide chemiluminescence monitors in a polluted urban environment, *Atmos. Chem. Phys.*, 2007, **7**, 2691–2704.

59 S. Zhou, C. J. Young, T. C. VandenBoer, S. F. Kowal and T. F. Kahan, Time-resolved measurements of nitric oxide, nitrogen dioxide, and nitrous acid in an occupied New York home, *Environ. Sci. Technol.*, 2018, **52**, 8355–8364.

60 J. Zhang and P. J. Lioy, Ozone in residential air: Concentrations, I/O ratios, indoor chemistry, and exposures, *Indoor Air*, 1994, **4**, 95–105.

61 K. Lee, J. Xue, A. S. Geyh, H. Ozkaynak, B. P. Leaderer, C. J. Weschler and J. D. Spengler, Nitrous acid, nitrogen dioxide, and ozone concentrations in residential environments, *Environ. Health Perspect.*, 2002, **110**, 145–150.

62 N. A. Mullen, J. Li, M. L. Russell, M. Spears, B. D. Less and B. C. Singer, Results of the California Healthy Homes Indoor Air Quality Study of 2011–2013: impact of natural gas appliances on air pollutant concentrations, *Indoor Air*, 2016, **26**, 231–245.

63 D. W. Dockery and J. D. Spengler, Indoor-outdoor relationships of respirable sulfates and particles, *Atmos. Environ.*, 1981, **15**, 335–343.

64 S. Madronich, Implications of recent total atmospheric ozone measurements for biologically active ultraviolet radiation reaching the Earth's surface, *Geophys. Res. Lett.*, 1992, **19**, 37–40.

65 B. Just, S. Rogak and M. Kandlikar, Characterization of ultrafine particulate matter from traditional and improved biomass cookstoves, *Environ. Sci. Technol.*, 2013, **47**, 3506–3512.

66 A. Leavey, S. Patel, R. Martinez, D. Mitroo, C. Fortenberry, M. Walker, B. Williams and P. Biswas, Organic and inorganic speciation of particulate matter formed during different combustion phases in an improved cookstove, *Environ. Res.*, 2017, **158**, 33–42.

67 E. Abt, H. H. Suh, G. Allen and P. Koutrakis, Characterization of indoor particle sources: A study conducted in the metropolitan Boston area, *Environ. Health Perspect.*, 2000, **108**, 35–44.

68 C. He, L. Morawska, J. Hitchins and D. Gilbert, Contribution from indoor sources to particle number and mass concentrations in residential houses, *Atmos. Environ.*, 2004, **38**, 3405–3415.

69 L. Wallace, Indoor sources of ultrafine and accumulation mode particles: Size distributions, size-resolved concentrations, and source strengths, *Aerosol Sci. Technol.*, 2006, **40**, 348–360.

70 C. Mohr, J. A. Huffman, M. J. Cubison, A. C. Aiken, K. S. Docherty, J. R. Kimmel, I. M. Ulbrich, M. Hannigan and J. L. Jimenez, Characterization of primary organic aerosol emissions from meat cooking, trash burning, and motor vehicles with high-resolution aerosol mass spectrometry and comparison with ambient and chamber observations, *Environ. Sci. Technol.*, 2009, **43**, 2443–2449.





71 Q. Zhang, J. L. Jimenez, M. R. Canagaratna, I. M. Ulbrich, N. L. Ng, D. R. Worsnop and Y. L. Sun, Understanding atmospheric organic aerosols via factor analysis of aerosol mass spectrometry: A review, *Anal. Bioanal. Chem.*, 2011, **401**, 3045–3067.

72 C. Mohr, P. F. DeCarlo, M. F. Heringa, R. Chirico, J. G. Slowik, R. Richter, C. Reche, A. Alastuey, X. Querol, R. Seco, J. Peñuelas, J. L. Jiménez, M. Crippa, R. Zimmermann, U. Baltensperger and A. S. H. Prévôt, Identification and quantification of organic aerosol from cooking and other sources in Barcelona using aerosol mass spectrometer data, *Atmos. Chem. Phys.*, 2012, **12**, 1649–1665.

73 L. Y. He, Y. Lin, X. F. Huang, S. Guo, L. Xue, Q. Su, M. Hu, S. J. Luan and Y. H. Zhang, Characterization of high-resolution aerosol mass spectra of primary organic aerosol emissions from Chinese cooking and biomass burning, *Atmos. Chem. Phys.*, 2010, **10**, 11535–11543.

74 T. Liu, Z. Wang, X. Wang and C. K. Chan, Primary and secondary organic aerosol from heated cooking oil emissions, *Atmos. Chem. Phys.*, 2018, **18**, 11363–11374.

75 A. M. Johnson, M. S. Waring and P. F. DeCarlo, Real-time transformation of outdoor aerosol components upon transport indoors measured with aerosol mass spectrometry, *Indoor Air*, 2017, **27**, 230–240.

76 J. D. Allan, P. I. Williams, W. T. Morgan, C. L. Martin, M. J. Flynn, J. Lee, E. Nemitz, G. J. Phillips, M. W. Gallagher and H. Coe, Contributions from transport, solid fuel burning and cooking to primary organic aerosols in two UK cities, *Atmos. Chem. Phys.*, 2010, **10**, 647–668.

77 P. R. Veres, J. M. Roberts, A. K. Cochran, J. B. Gilman, W. C. Kuster, J. S. Holloway, M. Graus, J. Flynn, B. Lefer, C. Warneke and J. de Gouw, Evidence of rapid production of organic acids in an urban air mass, *Geophys. Res. Lett.*, 2011, **38**, L17807, DOI: 10.1029/2011GL048420.

78 J. M. Mattila, P. Brophy, J. Kirkland, S. Hall, K. Ullmann, E. V. Fischer, S. Brown, E. McDuffie, A. Tevlin and D. K. Farmer, Tropospheric sources and sinks of gas-phase acids in the Colorado Front Range, *Atmos. Chem. Phys.*, 2018, **18**, 12315–12327.

79 R. Reiss, P. B. Ryan, S. J. Tibbetts and P. Koutrakis, Measurement of organic acids, aldehydes, and ketones in residential environments and their relation to ozone, *J. Air Waste Manage. Assoc.*, 1995, **45**, 811–822.

80 S. Liu, S. L. Thompson, H. Stark, P. J. Ziemann and J. L. Jimenez, Gas-phase carboxylic acids in a university classroom: Abundance, variability, and sources, *Environ. Sci. Technol.*, 2017, **51**, 5454–5463.

81 S. M. Duncan, S. Tomaz, G. Morrison, M. Webb, J. M. Atkin, J. D. Surratt and B. J. Turpin, Dynamics of residential water-soluble organic gases: Insights into sources and sinks, *Environ. Sci. Technol.*, 2019, **53**, 1812–1821.

82 J. N. Pitts, H. W. Biermann, E. C. Tuazon, M. Green, W. D. Long and A. M. Winer, Time-resolved identification and measurement of indoor air pollutants by spectroscopic techniques: Gaseous nitrous acid, methanol, formaldehyde and formic acid, *JAPCA*, 1989, **39**, 1344–1347.

83 H. Destaillats, M. M. Lunden, B. C. Singer, B. K. Coleman, A. T. Hodgson, C. J. Weschler and W. W. Nazaroff, Indoor secondary pollutants from household product emissions in the presence of ozone: A bench-scale chamber study, *Environ. Sci. Technol.*, 2006, **40**, 4421–4428.

84 A. Chebbi and P. Carlier, Carboxylic acids in the troposphere, occurrence, sources, and sinks: A review, *Atmos. Environ.*, 1996, **30**, 4233–4249.

85 A. Mielnik, M. Link, J. Mattila, S. R. Fulgham and D. K. Farmer, Emission of formic and acetic acids from two Colorado soils, *Environ. Sci.: Processes Impacts*, 2018, **20**, 1537–1545.

86 C. J. Weschler, Chemistry in indoor environments: 20 years of research, *Indoor Air*, 2011, **21**, 205–218.

87 M. Mendez, N. Blond, P. Blondeau, C. Schoemaecker and D. A. Hauglustaine, Assessment of the impact of oxidation processes on indoor air pollution using the new time-resolved INCA-Indoor model, *Atmos. Environ.*, 2015, **122**, 521–530.

88 V. W. Or, M. R. Alves, M. Wade, S. Schwab, R. L. Corsi and V. H. Grassian, Crystal clear? Microspectroscopic imaging and physicochemical characterization of indoor depositions on window glass, *Environ. Sci. Technol. Lett.*, 2018, **5**, 514–519.

89 R. Alwarda, S. Zhou and J. P. Abbatt, Heterogeneous oxidation of indoor surfaces by gas-phase hydroxyl radicals, *Indoor Air*, 2018, **28**, 655–664.

90 M. Kruza, A. C. Lewis, G. Morrison and N. Carslaw, Impact of surface ozone interactions on indoor air chemistry: A modeling study, *Indoor Air*, 2017, **27**, 1001–1011.

91 Y. Zhao, M. Hu, S. Slanina and Y. Zhang, The molecular distribution of fine particulate organic matter emitted from Western-style fast food cooking, *Atmos. Environ.*, 2007, **41**, 8163–8171.

92 K. L. Abdullahi, J. M. Delgado-Saborit and R. M. Harrison, Emissions and indoor concentrations of particulate matter and its specific chemical components from cooking: A review, *Atmos. Environ.*, 2013, **71**, 260–294.

93 E. Abt, H. H. Suh, P. Catalano and P. Koutrakis, Relative contribution of outdoor and indoor particle sources to indoor concentrations, *Environ. Sci. Technol.*, 2000, **34**, 3579–3587.

94 D. Lee and R. Condrate, FTIR spectral characterization of thin film coatings of oleic acid on glasses: I. Coatings on glasses from ethyl alcohol, *J. Mater. Sci.*, 1999, **34**, 139–146.

95 C. W. Spicer, D. W. Joseph and W. M. Ollison, A re-examination of ambient air ozone monitor interferences, *J. Air Waste Manage. Assoc.*, 2010, **60**, 1353–1364.